



**YACHAY UNIVERSITY OF EXPERIMENTAL
TECHNOLOGY AND RESEARCH**

SCHOOL OF CHEMICAL SCIENCE AND ENGINEERING

**Concentration and Composition of Ice Nucleating Particles in
Rain Water Samples from Quito, Mexico City, and Altzomoni.**

Trabajo de titulación presentado como requisito para la obtención del
título de Químico.

Author: DIANA LISSETH PEREIRA GUEVARA

dlpg1996@gmail.com

Advisors:

DR. LUIS ANTONIO LADINO MORENO

luis.ladino@atmosfera.unam.mx

DR. SANDRA PATRICIA HIDALGO BONILLA

sahidalgo@yachaytech.edu.ec

Urcuquí, August of 2019

Urcuquí, 22 de agosto de 2019

SECRETARÍA GENERAL
(Vicerrectorado Académico/Cancillería)
ESCUELA DE CIENCIAS QUÍMICAS E INGENIERÍA
CARRERA DE QUÍMICA
ACTA DE DEFENSA No. UITEY-CHE-2019-00003-AD

En la ciudad de San Miguel de Urcuquí, Provincia de Imbabura, a los 22 días del mes de agosto de 2019, a las 15:00 horas, en el Aula AI-101 de la Universidad de Investigación de Tecnología Experimental Yachay y ante el Tribunal Calificador, integrado por los docentes:

Presidente Tribunal de Defensa	Dra. SALUM , GRACIELA MARISA , Ph.D.
Miembro No Tutor	Mgs. LOPEZ ALCAÑIZ, MARTA
Tutor	Dra. HIDALGO BONILLA, SANDRA PATRICIA Ph.D.

Se presenta el(la) señor(ita) estudiante PEREIRA GUEVARA, DIANA LISSETH, con cédula de identidad No. 0804440246, de la ESCUELA DE CIENCIAS QUÍMICAS E INGENIERÍA, de la Carrera de QUÍMICA, aprobada por el Consejo de Educación Superior (CES), mediante Resolución RPC-SO-39-No.458-2014, con el objeto de rendir la sustentación de su trabajo de titulación denominado: Concentration and Composition of Ice Nucleating Particles in Rain Water Samples from Quito, Mexico City, and Altiplano., previa a la obtención del título de QUÍMICO/A.

El citado trabajo de titulación, fue debidamente aprobado por el(los) docente(s):

Tutor _____ Dra. HIDALGO BONILLA, SANDRA PATRICIA , Ph.D.

Y recibió las observaciones de los otros miembros del Tribunal Calificador, las mismas que han sido incorporadas por el(la) estudiante.

Previamente cumplidos los requisitos legales y reglamentarios, el trabajo de titulación fue sustentado por el(la) estudiante y examinado por los miembros del Tribunal Calificador. Escuchada la sustentación del trabajo de titulación, que integró la exposición de el(la) estudiante sobre el contenido de la misma y las preguntas formuladas por los miembros del Tribunal, se califica la sustentación del trabajo de titulación con las siguientes calificaciones:

Tipo	Docente	Calificación
Tutor	Dra. HIDALGO BONILLA, SANDRA PATRICIA , Ph.D.	10,0
Presidente Tribunal De Defensa	Dra. SALUM , GRACIELA MARISA , Ph.D.	10,0
Miembro Tribunal De Defensa	Mgs. LOPEZ ALCAÑIZ, MARTA	10,0

Lo que da un promedio de: 10 (Diez punto Cero), sobre 10 (diez), equivalente a: **APROBADO**

Para constancia de lo actuado, firman los miembros del Tribunal Calificador, el/la estudiante y el/la secretario ad-hoc.


PEREIRA GUEVARA, DIANA LISSETH
Estudiante


Dra. SALUM , GRACIELA MARISA , Ph.D.
Presidente Tribunal de Defensa


Dra. HIDALGO BONILLA, SANDRA PATRICIA , Ph.D.
Tutor


Mgs. LOPEZ ALCANIZ, MARTA
Miembro No Titular


ALVARADO AVILA, MARIA FERNANDA
Secretario Ad-hoc

AUTORIZACIÓN DE PUBLICACIÓN
AUTORÍA

Yo, **DIANA LISSETH PEREIRA GUEVARA**, con CI 0804440246 que las ideas, juicios, valoraciones, interpretaciones, consultas bibliográficas, definiciones y conceptualizaciones expuestas en el presente trabajo; así cómo, los procedimientos y herramientas utilizadas en la investigación, son de absoluta responsabilidad de el/la autor (a) del trabajo de titulación. Así mismo, me acojo a los reglamentos internos de la universidad correspondientes a los temas de honestidad académica.



Diana Lisseth Pereira Guevara
CI:0804440246

AUTORIZACIÓN DE PUBLICACIÓN

"Yo **DIANA LISSETH PEREIRA GUEVARA** cedo a la Universidad de Tecnología Experimental Yachay Tech, los derechos de publicación de la presente obra por un plazo máximo de cinco años, sin que deba haber un reconocimiento económico por este concepto. Declaro además que el texto del presente trabajo de titulación no podrá ser cedido a ninguna empresa editorial para su publicación u otros fines, sin contar previamente con la autorización escrita de la universidad"

Uruguay, Agosto de 2019



Diana Pereira

CI: 0804440246

ACKNOWLEDGMENTS

I would like to express my sincere and deep gratitude to my theses advisors Dr. Luis Ladino and Dr. Sandra Hidalgo, who gave me the opportunity to grow in the academic world. Thanks to Dr. Sandra Hidalgo for her patience, emotional and academic support, motivation and trust in my abilities. Thanks to Dr. Luis Ladino for his dedication, financial and academic support, for his tolerance and direction in the development of my theses project, and also for the opportunity to be part of his research team without previous knowledge of my aptitudes. I thank the Micro and Mesoscale Interaction group and the Atmospheric Sciences Centre from the UNAM for hosting me during my academic exchange in Mexico.

This thesis was financially supported by the Dirección General de Asuntos del Personal Académico (DGAPA) and by the Consejo Nacional de Ciencia y Tecnología (Conacyt) through grants PAPIIT IA108417 and CB-285023, respectively. Additional financial support was provided by Yachay Tech University through the resolution NRO.UITEY-CAN-2018-0073-M. I thank all three institutions because without their support it was impossible to execute the present project.

I also thank Dr. Rocío García, Eva Salinas, Leticia Martínez, Carlos Bermejo, Javier Juárez (UNAM), and Marlon Zambrano (Yachay Tech) for their collaboration in the experimental development of my theses.

Thanks to the dean of the School of Chemical Science and Engineering at Yachay Tech, Dr. Hortensia Rodríguez, and my professors Dr. Juan Pablo Saucedo, Dr. Kamil Makowski, and Dr. Filipe Areias for their academic support and comprehension during my academic exchange and the development of the project.

Thanks to my parents who always support me, for their dedication, advises, their constant love, and their motivation to improve myself.

DEDICATION

My experience at the University has been like a train, in which I have met many people, some of them have continued on the same route sharing careers and others had taken a different path, but each one of them left a teaching in me. My university life represents a stage of personal discovery that began when I left my comfort zone, called home, at this time I have grown emotionally, academically and above all humanly. I have learned that effort brings rewards, that one must learn to love what one does, and do it in the best way possible, I have learned to not be afraid of failure because it also leaves me teachings and make me stronger.

I admit that it has not been easy to get to this point, but now I feel a deep and authentic emotion for having completed a stage in the best way I think is possible and with the best effort I could do. Thinking about my professors, my friends, and all I learned in the University makes me feel nostalgic, but at the same time I know that my stage here is over and that I always will have good memories about Yachay Tech.

I want to dedicate my work to my parents Gladys and Angel. You are my principal motivation and the reason to make my best every day. This thesis is only one of the achievements that I hope to give you.

To my brothers Lincol and David.

Thanks to every person who have been part of my progress.

Resumen

Las partículas de aerosol pueden emitirse a la atmósfera y allí actuar como núcleos de congelación (INPs por sus siglas en inglés). Los INPs influyen en la formación de precipitación sobre los continentes y en el balance radiativo. Por esto, este trabajo estudia las habilidades para la formación de cristales de hielo de las partículas de aerosol que se encuentran en el agua de lluvia de Quito, Ciudad de México y Alzomoni. Para determinar la concentración y composición de los INPs en los sitios mencionados, se recolectaron muestras de agua de lluvia y se implementan las técnicas de congelación de gota y espectroscopia de absorción atómica. Se encontró que todas las muestras de aguas de lluvia presentan partículas de aerosol con habilidades nucleadoras de hielo. Pese a las diferencias entre Quito y México, los resultados obtenidos demostraron que las concentraciones y comportamiento de los INPs son similares y consistentes con la literatura. Contrario a esto, las muestras de Alzomoni indican mayor eficiencia en la formación de cristales de hielo. Finalmente, se establece que la correlación entre las concentraciones de los elementos Na^+ , K^+ , Mg^{2+} , Ca^{2+} y las habilidades nucleadoras de hielo de las partículas es muy baja.

Palabras Clave:

Aerosol, Partículas Nucleadoras de hielo, Nubes, Congelación Heterogénea, de lluvia, Composición Química.

CONTENT

1. TITLE	1
2. ABSTRACT.....	1
3. KEY WORDS.....	1
4. INTRODUCTION- JUSTIFICATION	2
4.1. THE ATMOSPHERE.....	2
4.2. AEROSOL PARTICLES	3
4.2.1. PRIMARY AND SECONDARY AEROSOL	3
4.2.2. ICE NUCLEATING PARTICLES	6
4.2.1.2. Freezing mechanisms of primary ice particles	7
4.2.1.3. Secondary Ice Particles	8
4.2.2. CHARACTERISTICS OF ICE NUCLEATING PARTICLES.....	9
4.2.2.1. Insolubility Requirement	9
4.2.2.2. Size Requirement	9
4.2.2.3. Chemical Bond Requirement.....	9
4.2.2.4. Crystallographic Requirement	9
4.2.2.5. Active Site Requirement	10
4.3. DETERMINATION OF INPS	10
4.3.1. LABORATORY STUDIES	10
4.3.2. FIELD (PORTABLE) STUDIES	10
4.4. CLOUDS	11
4.4.1. MIXED-PHASE CLOUDS.....	12
4.4.1.1. Hydrological cycle	12
4.4.1.2. Mixed-phase Clouds Formation.....	13
4.5. PRECIPITATION FORMATION.....	13
4.5.1. COLD RAIN	13
4.5.1.1. <i>Relationship between Precipitation Formation and the Presence of INPs</i>	14
5. PROBLEM STATEMENT	16
6. OBJECTIVES	18
6.1. GENERAL OBJECTIVE	18
6.2. SPECIFIC OBJECTIVES.....	18
6.3. HYPOTHESIS.....	18
7. METHODOLOGY	19

7.1. SAMPLING LOCATIONS DESCRIPTION	19
7.1.1. QUITO- ECUADOR	19
7.1.2. MEXICO CITY (CDMX)- MEXICO	20
7.1.2.1. Meteorological Conditions.....	21
7.1.3. ALTZOMONI (ALTZ), MEXICO STATE, MEXICO	21
7.1.3.1. Meteorological Conditions.....	22
7.2. SAMPLING METHOD.....	22
7.2.1. ECUADOR SAMPLING	22
7.2.2. MEXICO SAMPLING	23
7.3. DROPLET FREEZING ASSAY (DFA)	24
7.3.1. EQUIPMENT DESCRIPTION	25
7.3.2. SAMPLE PREPARATION	26
7.3.3. FREEZING SYSTEM DESCRIPTION	26
7.3.4. FREEZING EXPERIMENT	27
7.3.4.1. Standard Analysis.....	28
7.3.5. STATISTICAL ANALYSIS.....	29
7.3.5.1. Activation Curves.....	30
7.4. ATOMIC ABSORPTION SPECTROSCOPY	30
7.4.1. SAMPLE PREPARATION	30
7.4.2. EQUIPMENT DESCRIPTION	31
7.4.2.1. Hollow Cathode Lamps.....	32
7.4.2.2. Atomizer.....	33
7.4.2.3. Monochromator	33
7.4.2.4. Detector	33
7.4.3. ATOMIC ABSORPTION ANALYSIS	34
7.4.4. DATA ANALYSIS.....	34
7.5. HYSPLIT BACK-TRAJECTORIES.....	34
8. RESULTS AND DISCUSSION	36
8.1. DROPLET FREEZING ASSAY	36
8.1.1. DETERMINATION OF THE IDEAL CONDITIONS	36
8.1.2. URBAN CITIES COMPARISON	38
8.1.3. URBAN VS. RURAL LOCATIONS.	40
8.1.4. ICE NUCLEATING PARTICLES CONCENTRATION	43
8.2. ATOMIC ABSORPTION	44
8.2.1. CORRELATION BETWEEN IONS CONCENTRATION AND T ₅₀	45

8.3. BACK-TRAJECTORIES	47
8.3.1. QUITO	47
8.3.2. MEXICO CITY	48
8.3.3. ALTZOMONI.....	48
9. CONCLUSIONS AND RECOMENDATIONS.....	50
9.1. CONCLUSIONS	50
9.2. RECOMMENDATIONS.....	52
BIBLIOGRAPHY	

1. TITLE

Concentration and Composition of Ice Nucleating Particles in Rain Water Samples from Quito, Mexico City, and Altzomoni.

2. ABSTRACT

Aerosol particles which are emitted to the atmosphere by primary or secondary processes, can act as cloud condensation nuclei (CCN) and/or ice nucleating particles (INP) influencing cloud droplets and ice crystals formation, respectively. Therefore, aerosol particles are fundamental in the formation and modification of cold clouds and precipitation. This research studied precipitation samples from Mexico City (Mexico), Quito (Ecuador), and Altzomoni (Mexico) with the main objective of determining the concentration and composition of INPs to provide information about the role that aerosol particles play at tropical latitudes. Rain water samples were collected at different dates from July to November for Mexico City, and Altzomoni, and in June for Quito. Experimental analysis were performed with the Droplet Freezing Assay (DFA) and Flame Atomic Absorption Spectroscopy (FAAS) techniques. It was found that the three places under analysis were influenced by the presence of efficient INPs at concentrations in the range from 10^2 to 10^5 L⁻¹ water. Surprisingly, the ice nucleating abilities of the samples from Quito and Mexico City were comparable. The aerosol particles contained in the rural samples (i.e., from Altzomoni) were found to be more efficient INPs, in comparison with the particles contained in the urban samples (i.e., from Quito and Mexico City). The high ice nucleating abilities shown by the rural samples are likely related with the presence of biological particles such as bacteria. When correlating the ice nucleating abilities of the rain water samples with their chemical composition from the FAAS, poor correlation coefficients were obtained. The present results from the densely populated cities (i.e., urban) were found to be consistent with literature data from urban places at tropical latitudes.

3. KEY WORDS

Aerosol, Ice Nucleating Particles, Clouds, Heterogeneous Freezing, Rain water, Chemical Composition.

4. INTRODUCTION- JUSTIFICATION

4.1. THE ATMOSPHERE

The atmosphere is a gaseous layer which surrounds the Earth. It can be described in terms of layers that are defined based on altitude and average air temperature variations into Troposphere, Stratosphere, Mesosphere, and Thermosphere as shown in Figure 1.¹ The troposphere is the lowest layer of the atmosphere, ranging from the Earth's surface to an altitude of about 10–15 km (depending on the latitude), at which temperature decreases with altitude,² and where 80% of the total atmospheric mass is contained with contributions of gases and solid/liquid particles.

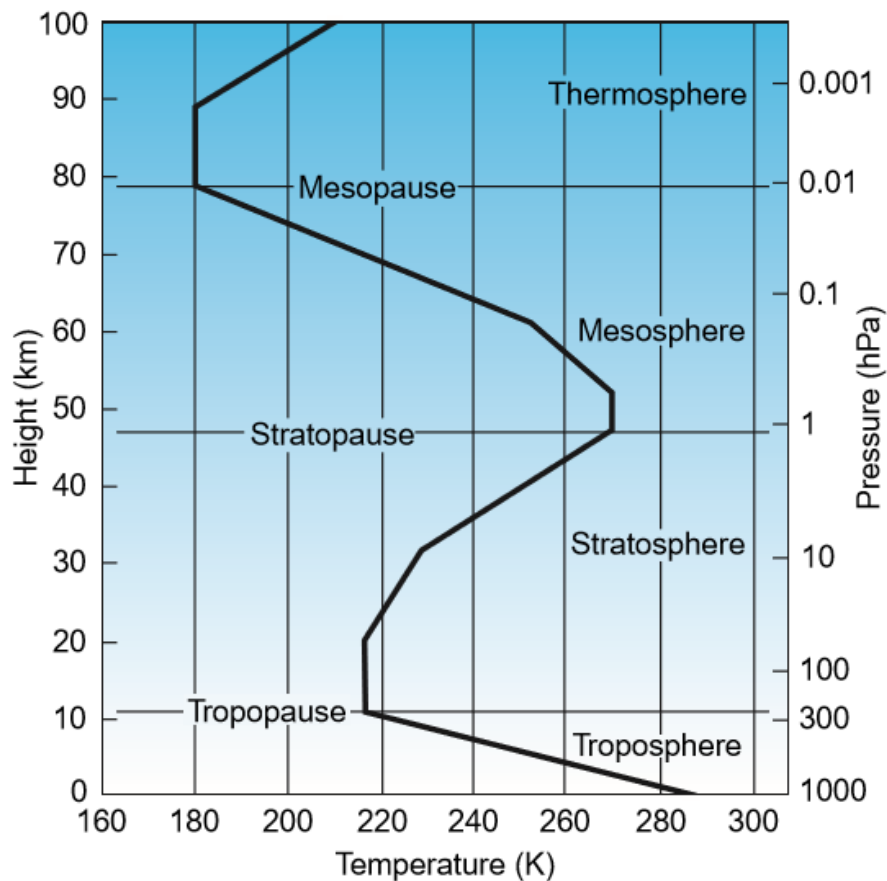


Figure 1. Vertical profile of the atmospheric layers on Earth's atmosphere¹.

4.2. AEROSOL PARTICLES

Aerosol refers to solid or liquid particles suspended in the atmosphere in which those play an important role in the modification of clouds³ and precipitation development⁴. Thus, they have important impacts on the hydrological cycle, the radiative balance of the planet, and the global climate.⁵

4.2.1. PRIMARY AND SECONDARY AEROSOL

Aerosol particles are classified as being of primary origin if they are directly emitted into the atmosphere from either natural sources (e.g., volcanic eruptions, sea spray, and erosion mechanisms) or anthropogenic processes (e.g., incomplete combustion of fossil fuels and industrial processes).⁶ Secondary aerosol particles are formed from precursor gases emitted in the atmosphere,⁷ through chemical reactions or physical transformations such as the nucleation of particles known as to gas-to-particle conversion or the condensation of vapor species on existing particles.⁸ Aerosol particles in the atmosphere usually cover a size range of several orders of magnitudes, from about 1 nm up to around 100 μm .⁹ They are divided into different modes according to their size as shown in Table 1.¹⁰

Table 1. Aerosol modes with their corresponding radius ranges¹⁰.

Aerosol mode	Range in radius
Nucleation mode	1.5 – 5 nm
Aitken mode	> 5 nm – 0.05 μm
Accumulation mode	> 0.05 – 0.5 μm
Coarse mode	> 0.5 – 5 μm
Giant particles	> 5 μm

Seinfeld and Pandis² explain that aerosol particles in the accumulation mode are the result of primary emissions or condensation and coagulation of secondary aerosol particles, while particles in the coarse mode are almost the product of mechanical process such as wind.

Furthermore, particles in the nucleation mode form by nucleation from supersaturated vapors emitted into the atmosphere such as volatile organic compounds (VOC), then those particles grow by condensation and coagulation to form Aitken and accumulation mode particles.¹⁰ From these modes, the dominant particles, in number, are those ranging between 0.001 μm and 1 μm as shown in Figure 2.

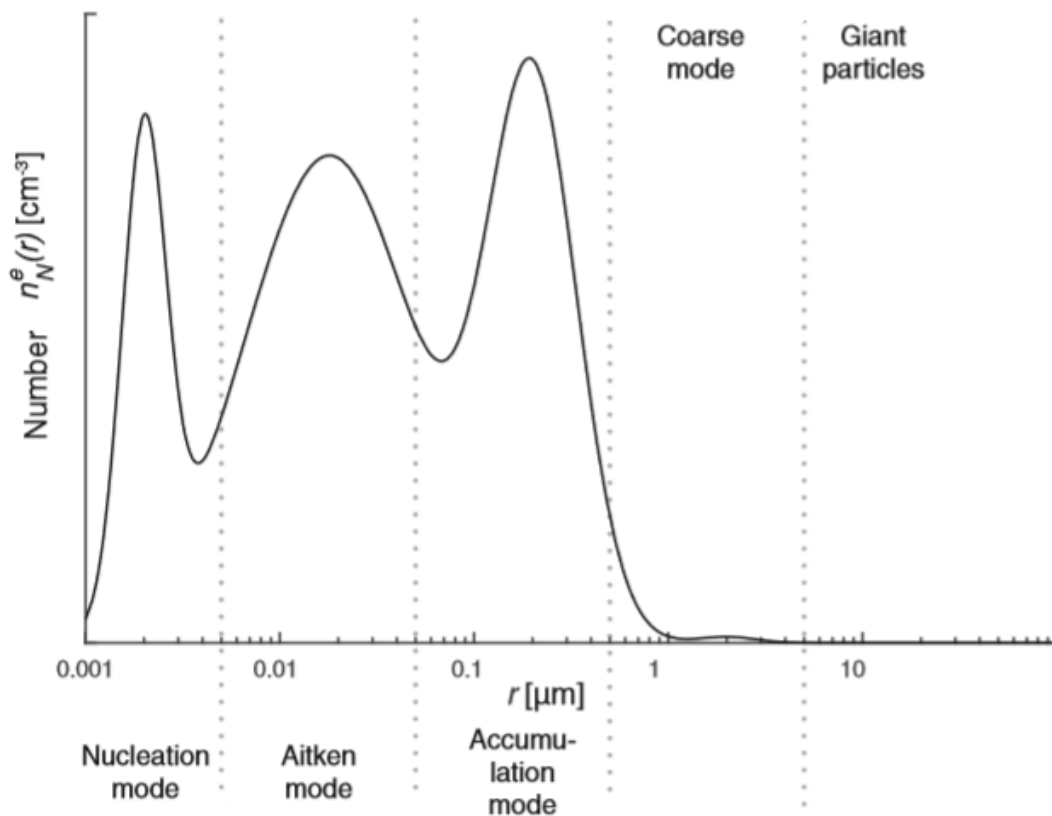


Figure 2. Size distribution of atmospheric aerosol particles.¹⁰

Some of the most abundant aerosol particles emitted correspond to: (1) sea salt; (2) soil dust; (3) inorganic salts (sulfate, nitrate, ammonium); (4) Organic Carbon (OC); (5) Elemental Carbon (EC); and (5) biological particles (e.g., bacteria, spores, pollen, fungi, viruses, among others).⁴

4.2.1.1. Removal of aerosol particles from the atmosphere

Figure 3 illustrates the different ways of production, growth, and removal of atmospheric aerosol particles.¹¹ The aerosol dynamics work under the influence of winds and are removed from the atmosphere either by impacting with the Earth's surface (dry deposition) or by being washed out by precipitating clouds (wet deposition).¹²

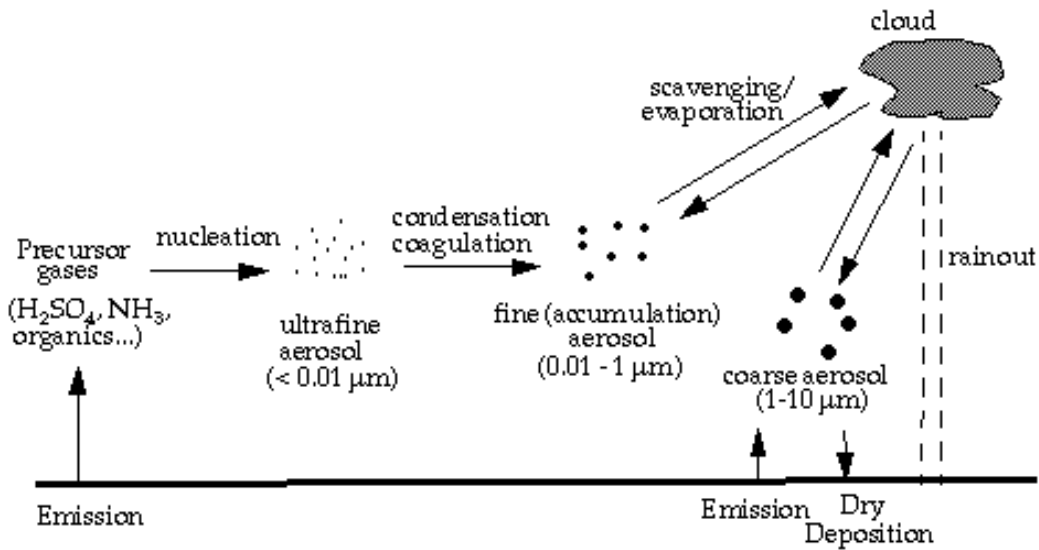


Figure 3. Aerosol particles emission, formation, and scavenging processes occurring in the atmosphere.¹¹

Wet deposition involves scavenging of aerosol particles by the interaction with precipitation and clouds, whereas dry deposition is related to direct collection of particles in the air, occurring by the action of turbulent diffusion, gravity, impaction, interception and Brownian diffusion.¹³ As shown in Figure 4, wet deposition will occur in different ways such as in-cloud scavenging where particles are captured by cloud droplets within the cloud, and below-cloud scavenging where particles in the air column below the cloud are incorporated into droplets due to impaction.¹⁴

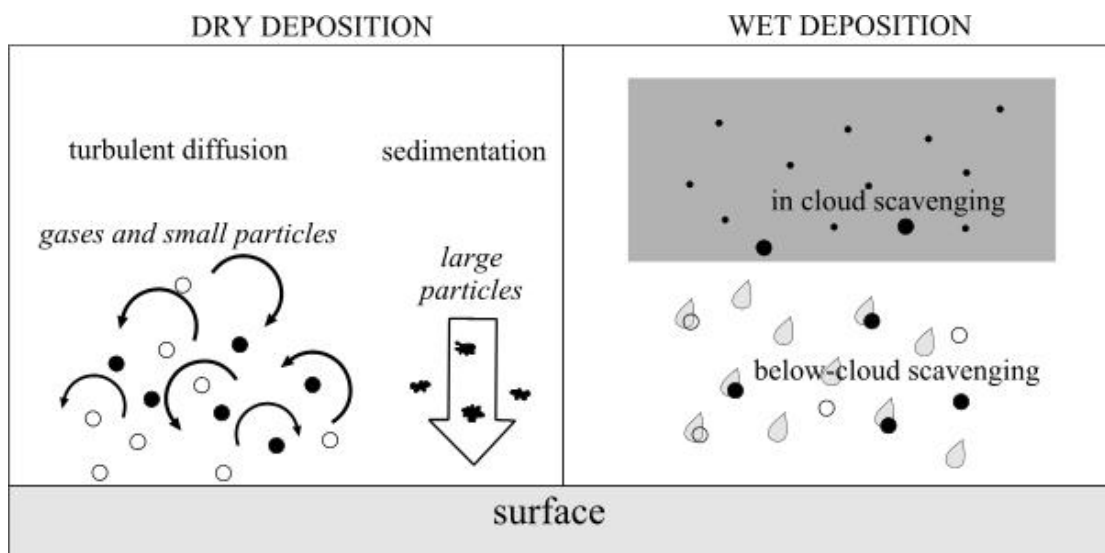


Figure 4. Dry and wet deposition occurring in the atmosphere.¹³

Furthermore, aerosol particles can act as cloud condensation nuclei (CCN) or ice nucleating particles (INPs), in order to facilitate the nucleation of liquid cloud droplets or induce the formation of ice crystals, respectively.¹⁵

4.2.2. ICE NUCLEATING PARTICLES

Nucleation implies a phase transition where a cluster of a thermodynamically stable phase forms and grows with the surrounding metastable parent phase and it occurs in two ways: homogeneously from aqueous droplets or heterogeneously from distinct aerosol particles at different thermodynamic conditions.¹⁶

In terms of temperature and relative humidity with respect to ice (RH_i), homogeneous freezing occurs below -38°C and $RH_i > 140\text{-}150\%$. In contrast, heterogeneous freezing, which requires INPs as a catalyst, occurs at temperatures warmer than -38°C and lower RH_i than those required for homogeneous freezing.¹⁷ Heterogeneous ice nucleation in the atmosphere is induced by INPs in different ways as shown in Figure 5: a) Deposition nucleation, b) Immersion freezing, c) Condensation freezing, and d) Contact freezing.¹⁸

4.2.1.2. Freezing mechanisms of primary ice particles

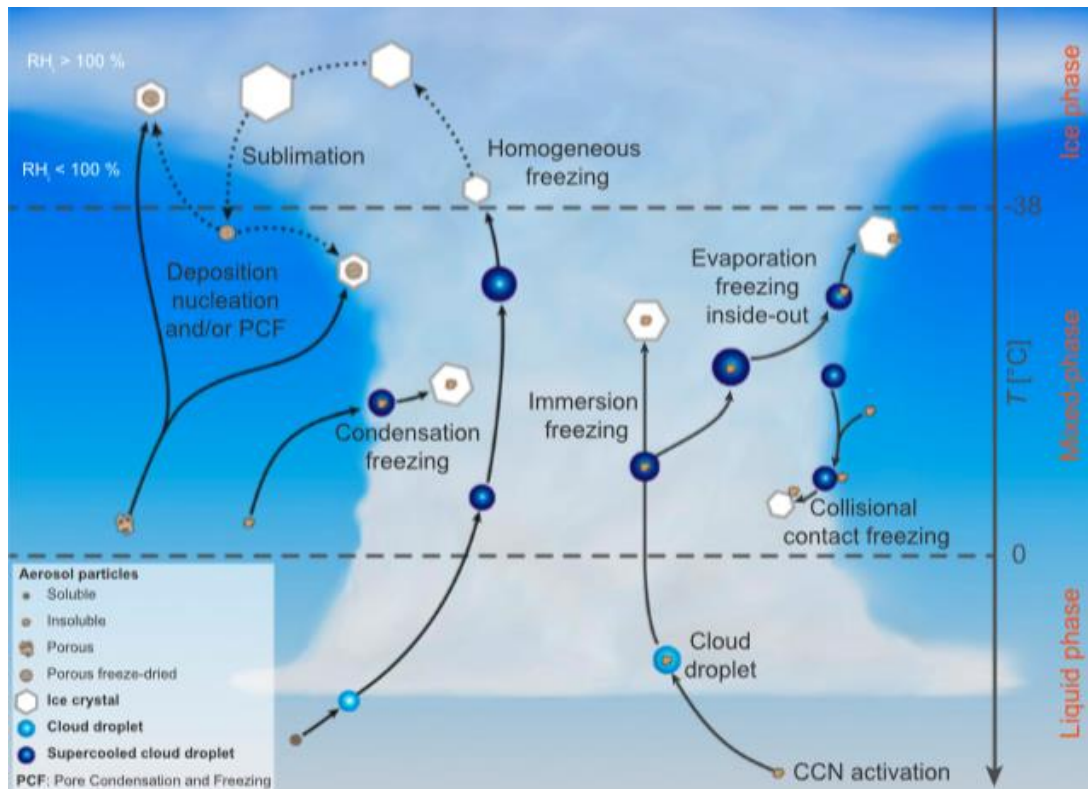


Figure 5. Freezing mechanisms for ice crystals formation.¹⁷

As can be seen in Figure 5, contact freezing occurs when an INP collides with the surface of a supercooled liquid droplet and ice nucleation occurs at the air-liquid-solid interface.¹⁹ Condensation freezing initiates by the formation of a liquid phase on a CCN at supercooled temperatures. Once the liquid phase is formed it automatically freezes.¹⁷ Murray et al.²⁰ explain that immersion freezing takes place when an INP is immersed into a liquid droplet, which is subsequently cooled to initiate ice formation. Finally, deposition nucleation takes place when the water vapor deposits directly on the surface of an INP to form the ice crystal, and it is the only heterogeneous mechanism where liquid water is absent.¹⁷ When and where in the atmosphere each mechanism takes place depend on the INP composition, ambient temperature, water supersaturation, among other factors.²¹

Once ice particles are formed, they can grow in the atmosphere by different mechanism such as: a) Growth from vapor deposition, b) Growth by riming, which refers to the increase in ice mass caused by the collision of ice particles with supercooled droplets that freezes right after the collision takes place, and c) Growth by aggregation, at which ice particles grow when they collide with other ice particles.²¹

4.2.1.3. Secondary Ice Particles

Secondary ice refers to the formation of ice crystals from preexisting ice without requiring the involvement of an INP.²² Secondary ice processes (SIP) acting in the formation of secondary ice were discovered due to the difference in the concentration of crystals and the concentration of measured INPs, which was believed to be on the same order, but experimental data showed that within natural clouds the concentration of ice crystals exceeds the concentration of INPs by several orders of magnitude.²³

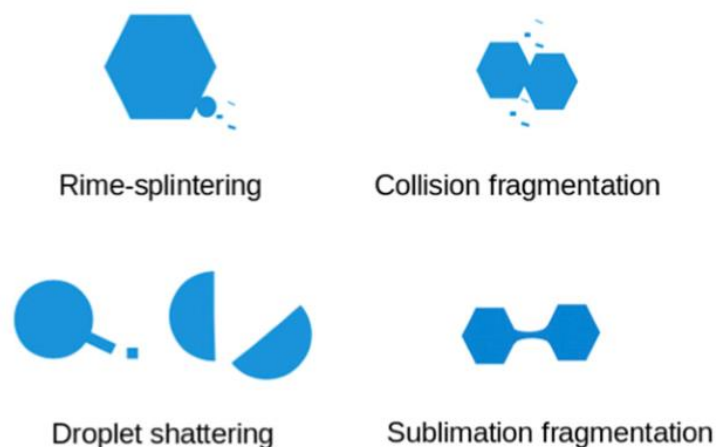


Figure 6. Secondary Ice processes.²²

Figure 6 shows the four proposed mechanisms in the formation of secondary ice. Those are: rime splintering, proposed by Hallett and Mossop,²³ droplet shattering where splinters are produced from the freezing of supercooled droplets,²⁴ crystal-crystal collision fragmentation,²⁵ and sublimation fragmentation,²⁶ in which ice fragments separate from the parent particle during sublimation process.

4.2.2. CHARACTERISTICS OF ICE NUCLEATING PARTICLES

Only a small fraction of the aerosol particle's population can act as INP, ranging from 10^0 to 10^{10} L^{-1} water.³ In that way, to have aerosol particles acting as INPs, some features are required:

4.2.2.1. *Insolubility Requirement*

INPs should be water insoluble because soluble particles follow a tendency to disintegrate under the action of water and the ice germ formation is avoided.²¹ Ansmann et al.²⁷ suggest that aerosol particles contain insoluble and soluble components, and that the insoluble part is responsible for heterogeneous ice formation.

4.2.2.2. *Size Requirement*

Diehl and Wurzler²⁸ demonstrated in laboratory studies that there is a correlation between the freezing ability of an aerosol particle and its size. Therefore, larger aerosol particles are considered more efficient INPs because the concentration of INPs active at temperature warmer than -20°C is proportional to the concentration of large particles.²¹ Moreover, DeMott and coworkers²⁹ state that the concentration of INPs can be explained by the concentration of aerosol particles larger than $0.5 \mu\text{m}$.

4.2.2.3. *Chemical Bond Requirement*

Good INPs must have available hydrogen bonds at their surface because the ice crystal lattice is held together by hydrogen bonds.²¹

4.2.2.4. *Crystallographic Requirement*

Lohmann et al.¹⁶ stated that a crystalline structure similar to that of ice is preferable because water molecules can easily form an ice lattice on them.

4.2.2.5. *Active Site Requirement*

Pruppacher and Klett²¹ explained that heterogeneous nucleation is a localized phenomenon, so it proceeds at distinct active sites on a substrate surface. Indeed, good INPs present many active sites capable of absorbing water molecules to initiate ice nucleation. Active sites refer to areas where initiating ice nucleation is easily.³⁰

4.3. DETERMINATION OF INPS

Different methods to study ice nucleation have been developed since 1940 due to the increasing necessity of analyzing the INP concentrations³¹ to explain the formation of ice crystal, which play an important role in the precipitation formation.²³

4.3.1. LABORATORY STUDIES

There are several laboratory studies that currently use non-portable systems to investigate INPs, which according to Cziczo et al.³² are motivated due to the ice nucleating abilities presenting on some samples without condensible connection to atmospheric abundance. For that reason, some methods have been developed such as wind tunnel experiments, droplet levitation²⁶, optical microscope³³, cloud chamber methods,^{34,35} and freezing experiments, in which this study will focus. Freezing experiments were introduced by Bigg³⁶ and Vali³⁷, who analyzed the precipitation through the freezing of water drops to obtain a nucleus spectra and derive the concentration of INPs at specific temperature ranges. More recently, Cascajo³⁸, DeMott et al.³⁹, among others, applied freezing experiments to simulate immersion freezing because this mechanism is the key process occurring in the formation of ice crystals in mixed-phase clouds.

40

4.3.2. FIELD (PORTABLE) STUDIES

In the same way that for laboratory experiments, in field studies, portable chambers can be used to quantify ice crystal³², differing in the size of the instruments. Additionally, Rogers⁴¹ introduced the use of radars (acoustic, microwaves), and lasers to detect ice crystals in atmosphere, which can be correlated with the presence of INPs.

4.4. CLOUDS

According to the World Meteorological Organization (WMO), clouds are an aggregate of cloud droplets or ice crystals, or a combination of both, suspended in air⁴². Figure 7 shows that they can be classified according to their cloud base height into high, mid-, and low-level clouds.¹⁶ High-level clouds use the prefix cirrus, which indicates clouds located above 7 km, which mainly consists of ice crystal due to the low air temperatures. Mid-level clouds use the prefix alto- which denotes clouds with cloud bases in the mid-troposphere between 2 and 7 km. Hence, mid-level clouds consist of droplets and ice crystals. Finally, low-level clouds are formed of cloud droplets only and they are usually below 2 km.⁴³

Other classification can be achieved according to cloud microphysical properties (phase of contained hydrometeors, which are particles leaving the cloud) into warm, cold and mixed-phase clouds. Warm clouds mainly consist of liquid water in the form of cloud droplets. Analogously, cold clouds consist mostly of ice crystals.¹⁵ If clouds contain a mixture of ice crystals and cloud droplets, they are denoted as mixed-phase clouds and they can typically be found at temperatures ranging between 0 and -38°C .¹⁷

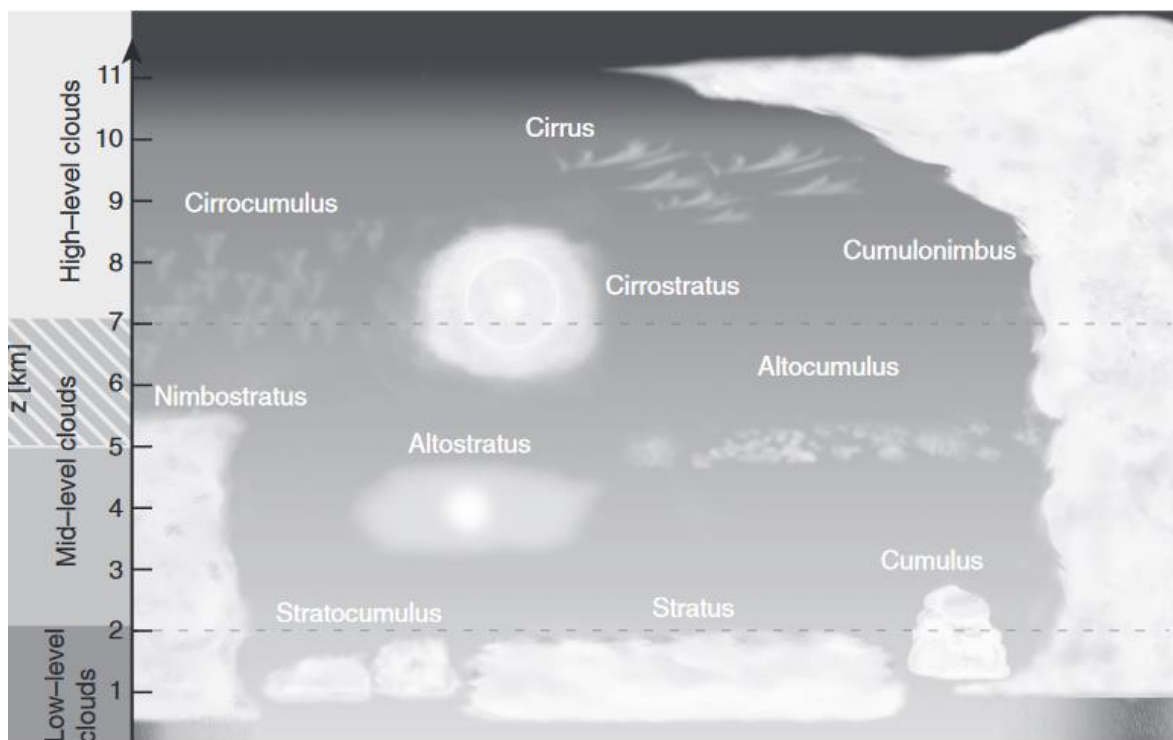


Figure 7. Clouds classification based on the cloud base height in the troposphere.¹⁶

4.4.1. MIXED-PHASE CLOUDS

These clouds are characterized by the complex interactions between water vapor, liquid, and ice in the same system.⁴⁴ Mixed-phase clouds can be found at all latitudes from polar regions to the tropics. De Boer et al.⁴⁵ explain that there is an important liquid-ice dependence in mixed-phase clouds due to their structure, thus, this dependence explains that clouds composed of ice crystals and liquid droplets are more frequently than clouds composed entirely of ice.

Analyzing the formation of mixed-phase cloud is the focus of the present study because their widespread nature allows them to play critical roles in the life time of clouds, efficiency at reflecting radiation, and in precipitation formation.⁴⁶ At the same time, these roles influence the hydrological cycle.⁴⁷

4.4.1.1. Hydrological cycle

The hydrological cycle represents a continuous series of processes occurring simultaneously that allows the movement of water between and within the atmosphere and the Earth's surface.⁴⁸ In the review "*Understanding of Earth's Hydrological cycle*", the authors Rast et al.⁴⁹ argue that the hydrological cycle is composed of different mechanisms of transport, which include evaporation from water and soil surfaces, evapotranspiration from vegetated land, transport of water vapor in the atmosphere related to cloud dynamics, the mechanisms leading to liquid and solid precipitation, the movement of water in soil by root dynamics, river run-off, and groundwater flow (See Figure 8).

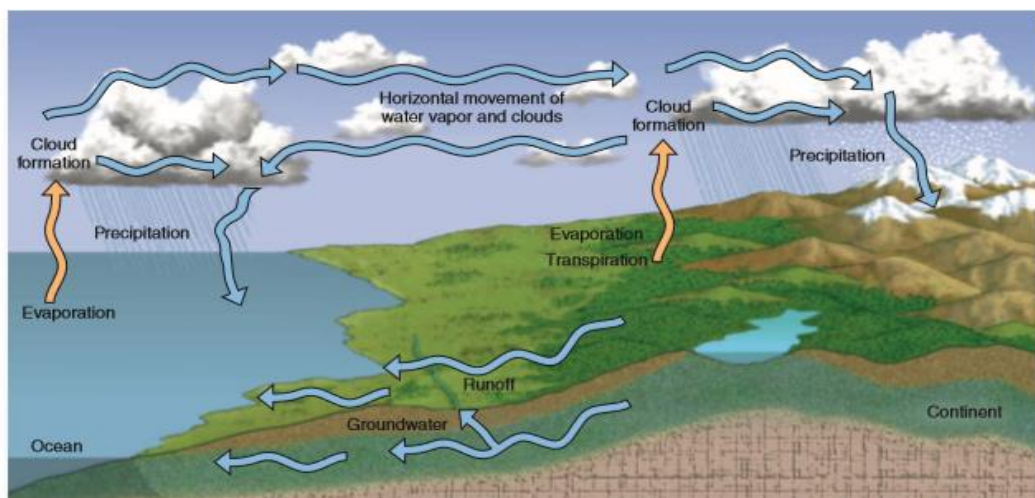


Figure 8. Hydrological Cycle representation through atmosphere, water, and land interactions.⁴⁸

4.4.1.2. *Mixed-phase Clouds Formation*

Mixed-phase clouds can be formed in the atmosphere due to adiabatic cooling of ascending parcels⁵⁰ or by the activation of liquid water within a preexistent ice cloud⁵¹. In the former process, inside the updrafts, liquid cloud droplets form by CCN activation, and ice crystals are produced from INPs by the different heterogeneous mechanism as described above.⁴⁶ In contrast, the activation of liquid water to transform an ice cloud into a mixed cloud phase consider three routes: uniform ascent, harmonic vertical oscillations, and turbulent fluctuations.⁵¹ The first two represent motions in the vertical limited in time and space, and the third scenery is associated to the turbulence generated by the vertical motions in clouds.

4.5. PRECIPITATION FORMATION

Precipitation gives origin to warm and cold rain, where precipitation represents hydrometeors consisting of an ensemble of particles falling down, and rain is a type of precipitation of drops of water which falls from a cloud.⁴² Warm and cold rain differ in their thermodynamic phase components. Mülmenstädt et al.⁵² describes that if the thermodynamic phase at the cloud top is ice or mixed-phase, precipitation is classified as cold rain, and if it is liquid and no ice is present, the precipitation is considered as warm rain.

4.5.1. COLD RAIN

Cold rain formation in mixed-phase clouds can be explained by the Wegener-Bergeron-Findeisen process (See Figure 9). Wegener⁵³ proposed a theory of ice crystal growing due to a difference in water vapor saturation between ice crystals and liquid water droplets. Then, Bergeron⁵⁴ hypothesized that most rain-drops begin as ice crystals in supercooled cloud where they grow at expenses of evaporating drops. With the contribution of Wegener and Bergeron, Findeisen⁵⁵, stated that ice crystals grow by vapor deposition coming from supercooled liquid droplets due to a difference in saturation vapor pressure, which is lower for ice crystals than liquid water. Because the saturation vapor pressure of liquid water is higher than ice, the evaporation rate at cloud droplets is higher than condensation. Thus, the produced vapor molecules are deposited onto the crystals surface, which grow and precipitate.⁵⁶

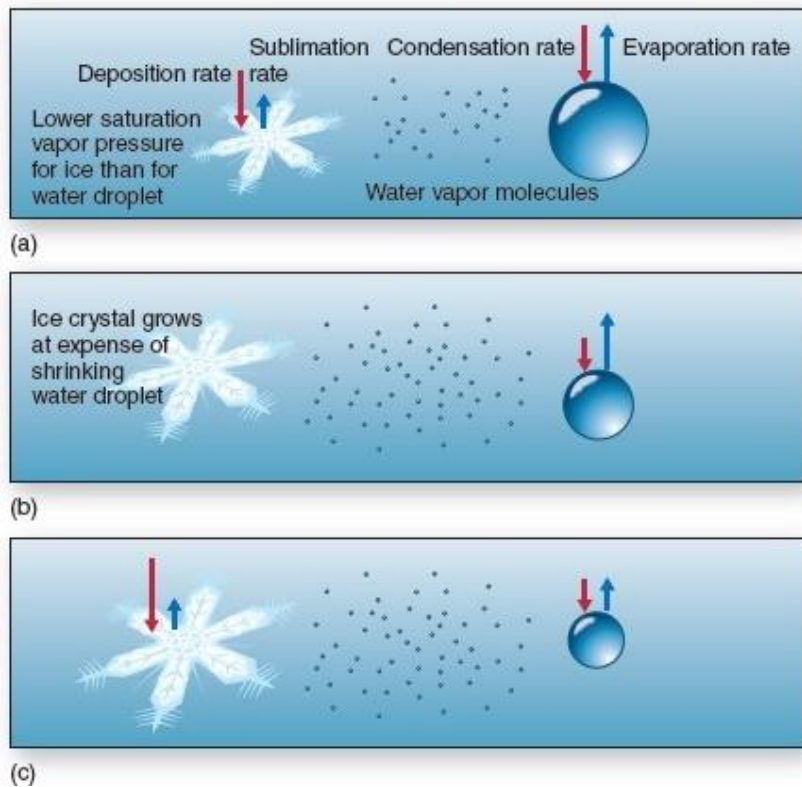


Figure 9. Wegener-Bergeron-Findeisen process: explains precipitation formation via the ice phase.⁴⁸

4.5.1.1. Relationship between Precipitation Formation and the Presence of INPs

Considering that most of the precipitation over the continents occurs via the ice phase,⁵² the presence of ice particles in clouds is fundamental in the formation of precipitation, the radiative properties of clouds, and the chemical interactions within clouds⁴.

In that way, DeMott et al.²⁹ show that more precipitation is formed when the concentration of INP is higher in mid-level clouds as shown in Figure 10. Supporting this idea, Knopf et al.⁵⁷ state that in mixed-phase clouds, the existence of ice crystals, which are related to the presence of INPs, may govern precipitation, which affects the hydrological cycle.

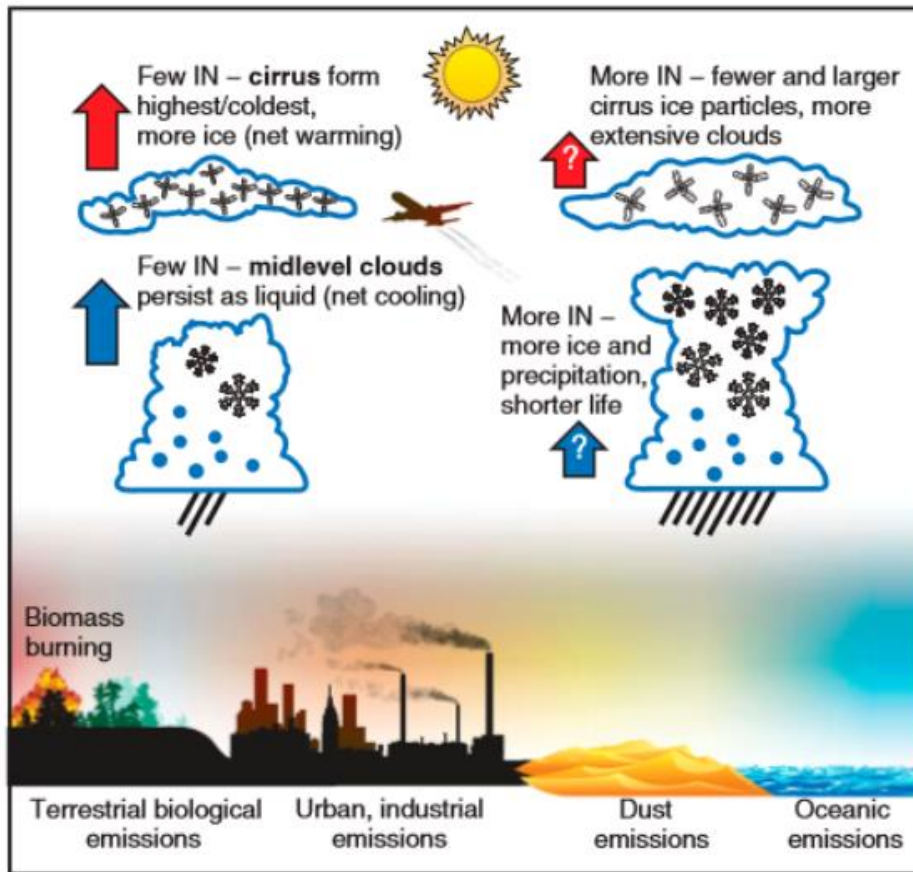


Figure 10. Illustration of the effect of ice crystals in cold clouds to form cold rain ²⁹

5. PROBLEM STATEMENT

The analysis of INPs tries to develop a better knowledge of atmospheric process that influence clouds and precipitation formation, which affects the planetary radiative balance, and the hydrological cycle. For these reasons, in the last decades there have been an increasing interest on analyzing the chemical composition, structural properties, and origin of aerosol particles in relation with their ice nucleating abilities. A recent study where a revision of old measurements of INPs present in precipitation samples, came out with a nucleus spectrum obtained from cloud water, rain water, snow, melted sleet, and hail samples as shown in Figure 11.

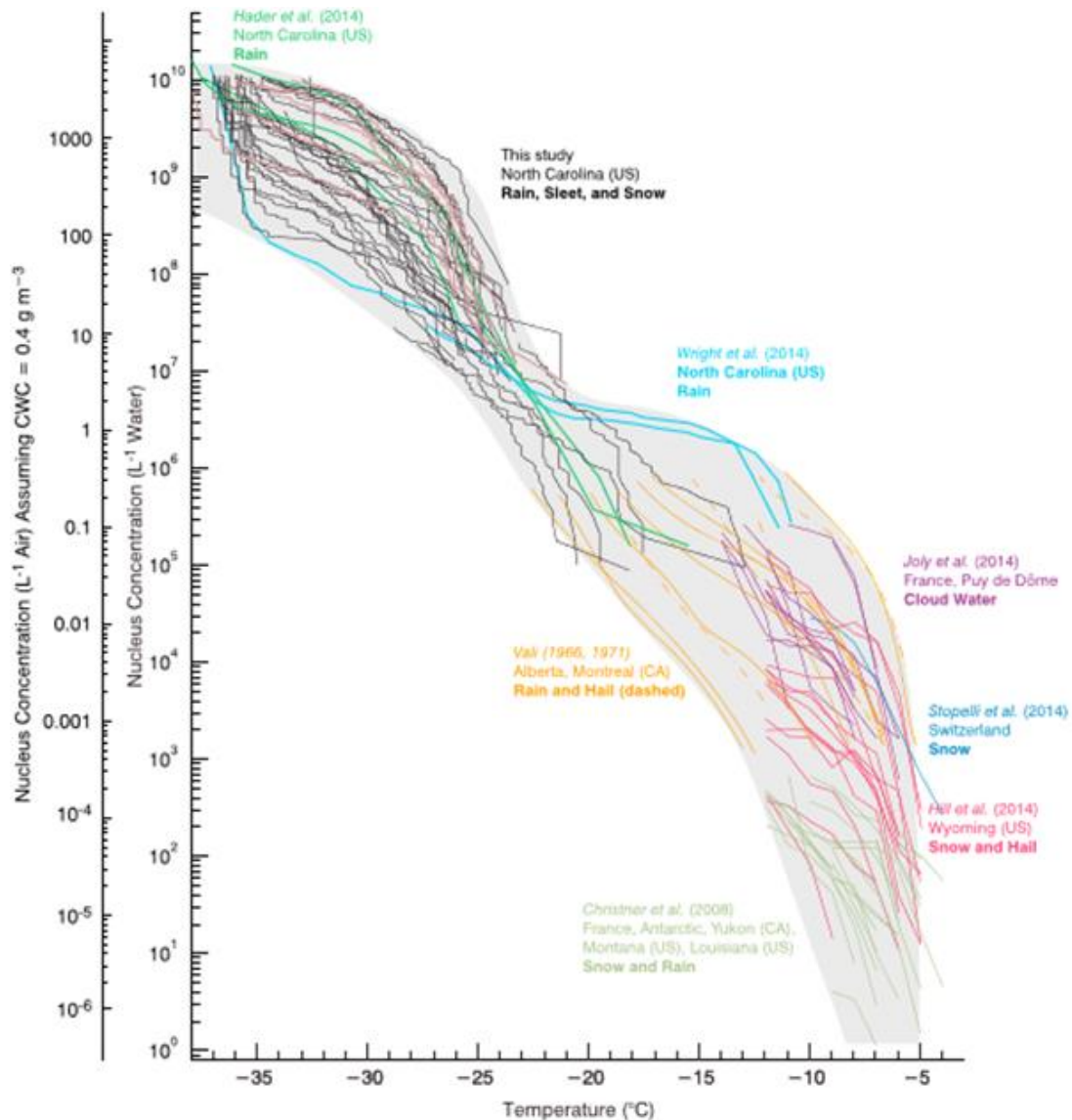


Figure 11. Nucleus spectrum from precipitation samples.³

The majority of the scientific studies on ice nucleation have been conducted in mid- and high-latitudes with little information from the tropics. In Mexico, few studies such as Ladino et al.⁵⁸ and Knopf et al.⁵⁷ talk about the sources of INPs from urban and maritime sources, whereas in Ecuador there are not studies reporting the characterization of INPs. In that way, it is clear that there is not enough information about INPs in those tropical places. Hence, studies similar to the present work are required to analyze rain water samples in order to understand aerosol's particles emission and the role that this phenomenon has in the cold clouds formation and precipitation patterns in the tropics.

To provide information about INPs and their role in the precipitation patters, freezing analysis and atomic absorption analysis will be performed to determine the ice nucleating abilities of the aerosol particles contained in the rain samples.

6. OBJECTIVES

6.1. GENERAL OBJECTIVE

To study the concentration and composition of ice nucleating particles in rain water from Quito, Mexico City, and Alzomoni.

6.2. SPECIFIC OBJECTIVES

- To determine the freezing temperature of precipitation samples through the Droplet Freezing Assay analysis and to compute the concentration of INPs present on them.
- To determine the chemical composition of rain water samples from different cities by performing atomic absorption analysis.
- To establish the relationship between INPs and precipitation patterns in two densely populated tropical cities and one rural site by means of Back-trajectories.

6.3. HYPOTHESIS

There is a difference in the nucleating abilities of rain water samples from the urban cities of Quito and Mexico City.

7. METHODOLOGY

7.1. SAMPLING LOCATIONS DESCRIPTION

The sampling locations were chosen to provide information about two different tropical countries. Samples were collected in Quito, Mexico City (CDMX), and Altzomoni (ALTZ). Two of the places are related to urban locations (i.e., Quito and CDMX), whereas one of them can be considered as a rural location (i.e., ALTZ).

Rain water samples were collected at dates from June to November of 2018. The number of samples collected at each location is summarized in Table 2, and those are associated to different precipitation events.

Table 2. Collection dates of rain water samples. CDMX refers to Mexico City, while ALTZ to Altzomoni.

Samples			
Location	Quito	CDMX	ALTZ
Number	4	10	10

7.1.1. QUITO- ECUADOR

In Quito, samples were collected in the center of the city, in a house with a geographic location of 0.19°N and 78.51°W and an altitude of 2850 m.a.s.l. This place is surrounded by buildings and houses as shown in Figure 12, and is influenced by vehicular and urban emissions.



Figure 12. Sampling location in Quito.

The dates in which samples were collected in Quito are shown in Table 3. In the first sampling day the conditions were high cloudiness and heavy rain. In contrast, the three other samples were collected during the night with higher wind speed values, and the presence of moderate rain. There are not official meteorological conditions reported for these sampling days due to the lack of equipment.

Table 3. Data from rain water samples in Quito.

Sample	Date
ECUA 1	01/06/2018
ECUA 2	27/06/2018
ECUA 3	28/06/2018
ECUA 4	29/06/2018

7.1.2. MEXICO CITY (CDMX)- MEXICO

This sampling place is located at the Atmospheric Science Center (CCA) at the National Autonomous University of Mexico (UNAM), with a geographic location of 19.3262°N and 99.1761°W and an altitude of 2 280 m.a.s.l. Figure 13 shows the CCA station, which is influenced by the presence of vegetation and anthropogenic pollution.



Figure 13. Sampling station in Mexico City.⁵⁹

7.1.2.1. Meteorological Conditions

The samples were collected during the fall (September 23rd to December 21st) at temperatures below 18°C, and with meteorological conditions showing that samples were collected during light and moderate rain events, with light wind speeds associated. The data of the different meteorological variables during sample collection in CDMX are presented in Table 4.⁵⁹

Table 4. Data from rain water samples for Mexico City.

Sample	Date	Average temperature (°C)	Wind speed (km/h)	Precipitation (mm)
1	27/09/2018	16.51	4.95	8.00
2	28-30/09/2018	16.86	5.92	-
3	05-07/10/2018	16.31	6.00	25.02
4	10/10/2018	17.24	5.92	-
5	11/10/2018	17.75	5.40	15.00
6	12-14/10/2018	null	null	5.60
7	19-21/10/2018	15.56	6.62	15.00
8	26-28/10/2018	16.17	6.75	6.80
9	31/10-04/11/2018	14.87	5.06	8.00
10	13-14/11/2018	10.53	6.93	16.20

7.1.3. ALTZOMONI (ALTZ), MEXICO STATE, MEXICO

This place is located in the National Park Izta-Popo with a geographical location of 19.1187°N, and 98.6552°W in Altzomoni and at an altitude of 3 985 m.a.s.l. This station showed in Figure 14 is surrounded by a pine forest, and an active volcano (Popocatepetl), then, is likely influenced by biological aerosol emissions, and probably local mineral dust and ash particles.



Figure 14. Sampling station in Altzomoni.⁵⁹

7.1.3.1. Meteorological Conditions

The rain water samples in ALTZ were collected during the summer and fall seasons at different dates and cold temperatures (below 5°C). The meteorological conditions for ALTZ shown in Table 5,⁵⁹ indicate that samples were collected in the presence of gentle and moderate winds, with more intense precipitation events in comparison to CDMX and Quito.

Table 5. Data from rain water samples in Altzomoni.

Sample	Date	Average temperature (°C)	Wind speed (km/h)	Precipitation (mm)
1	14-20/06/2018	null	null	62.00
2	21-27/06/2018	3.30	13.19	32.20
3	14-19/08/2018	5.17	21.20	30.00
4	01-09/10/2018	3.91	11.73	15.60
5	Non reported	-	-	-
6	10-16/10/2018	5.34	22.31	31.00
7	17-21/10/2018	4.09	28.82	23.00
8	22-28/10/2018	4.03	27.06	6.30
9	07-13/11/2018	4.24	12.41	17.50
10	14-18/11/2018	3.16	10.68	21.00

7.2. SAMPLING METHOD

The procedure performed to collect the samples varied between the countries due to the availability of resources. In Mexico, the samples were picked up by a Meteorological Institution from the UNAM that own the required equipment to collect precipitation samples, whereas the samples from Ecuador were taken by a student without the ideal equipment. The details will be explained in detail in the next section.

7.2.1. ECUADOR SAMPLING

An assembly of a graduated cylinder, and a funnel as is illustrated in Figure 15 was implemented to collect the rain samples in Quito. Four samples with a volume of 100mL were collected, and placed in four different amber bottles of 250mL.

Afterwards, 1mL of chloroform was added with a 1mL pipette to each bottle, with the main purpose of inhibiting bacteria proliferation. The samples were stored during one month at -20°C, and later on transported from Ecuador to México in a cooler. In México, prior to their analysis, they were stored at -26°C.



Figure 15. Experimental assembly to collect rain water sample.

7.2.2. MEXICO SAMPLING

Rain water samples in CDMX and ALTZ were collected by using a white bucket connected to a sensor. The bucket was covered with a metallic screen that opened when the intensity of sun light decreases and the cloudiness increases, which is generally associated to precipitation. From Figure 16 different parts of the setup can be identified. a) the sensor sensitive to sun light with a metallic assembly, which is displaced to open or close the metallic cover, b) and d) the whole assembly implemented to collect the rain water samples, and c) the metallic cover open and ready to sample.

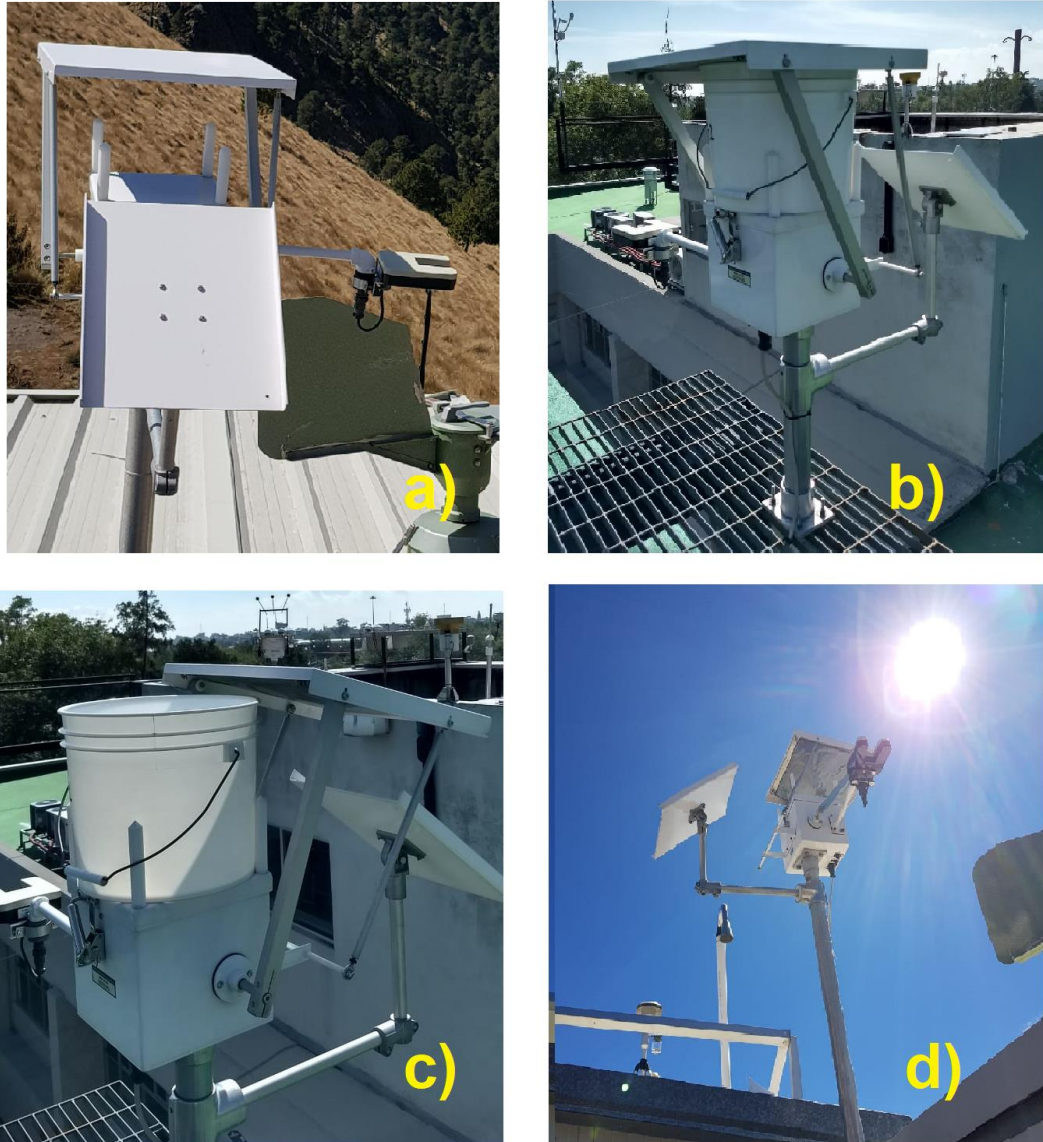


Figure 16. Experimental equipment implemented at the CDMX and Altzomoni stations to collect rain water.

When the container was full, it was transported to the CCA. From the bulk sample, 25mL of each sample were used to perform the ice nucleation analysis, and they were stored in refrigeration at 4°C prior to the analysis.

7.3. DROPLET FREEZING ASSAY (DFA)

The droplet freezing experiment allows us to study heterogeneous ice nucleation in small droplets, normally in the range of microliters.³⁸ The idea of this technique is to simulate the immersion freezing mechanism occurring in mixed-phase clouds because it is well known that

immersion freezing is the predominant mechanism of heterogeneous freezing occurring in this type of clouds²⁸. To achieve this process, the DFA was used as follows.

A DFA was recently built in the Micro and Mesoscale Interaction group of the CCA by a former undergraduate student. The DFA was originally designed by Vali³⁷; however, the used system in the present work is based on the design shown in Cascajo³⁸ and it is described in more detail in Juarez⁶⁰.

7.3.1. EQUIPMENT DESCRIPTION

The thermostat LAUDA PRO-RP 1090 is an equipment that works under the principle of a cold bath, regulating the temperature in a working temperature range from -90°C to 200°C with a temperature stability of $\pm 0.01^\circ\text{C}$.⁶¹ As shown in Figure 17, the internal structure of this equipment has two temperature sensor, and a pump, while the external component is a temperature control screen, which allows the users to vary the system temperature and to provide information about the temperature read by the two sensors.⁶²

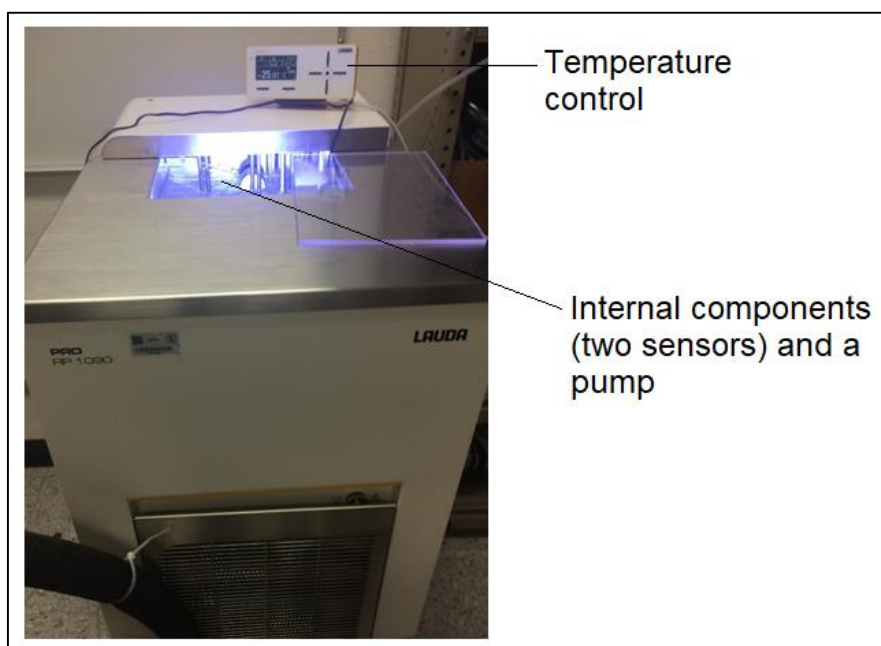


Figure 17. Thermostat LAUDA PRO-RP 1090

7.3.2. SAMPLE PREPARATION

Given that the Quito samples were frozen, prior to their analysis they were thawed at room temperature in a water bath and manually stirred to homogenize the sample. This was not necessary for the CDMX and ALTZ samples given that they were liquid prior to their analysis. Afterwards, using an eight tips micropipette of 100 μ l, shown in Figure 18, volumes of 50 μ l of sample were deposited in each of the 96 holes of an Elisa plate, and covered with a transparent foil to avoid external contamination. This volume simulates the volume of a liquid rain drop with a size of ca. 4.4 mm, and therefore, we assume that each hole represents a liquid droplet with aerosol particles immersed on them, those of which were captured either by in-cloud or below-cloud scavenging.



Figure 18. Elisa Plate, Micropipette of eight points of 100 μ l and tips (Materials for sample preparation)

7.3.3. FREEZING SYSTEM DESCRIPTION

To perform an ice nucleation experiment using a DFA an assembly illustrated in Figure 19 was used. This consisted of a thermostat, a sample holder, a video recorder, and a light system. In the thermostat, a cooling liquid was introduced, this was polydimethylsiloxane, which works in a temperature range of -50 $^{\circ}$ C to 200 $^{\circ}$ C, and is used due to its good chemical stability and electrical insulating property.⁶³ Another component was the sample holder, in which the sample contained in the Elisa plate was incorporated to be in contact with the cooling liquid.

Additionally, a led lamp was added to the system to allow the visualization of the freezing experiments that was be recorded by a camera located at the top of the sample holder.

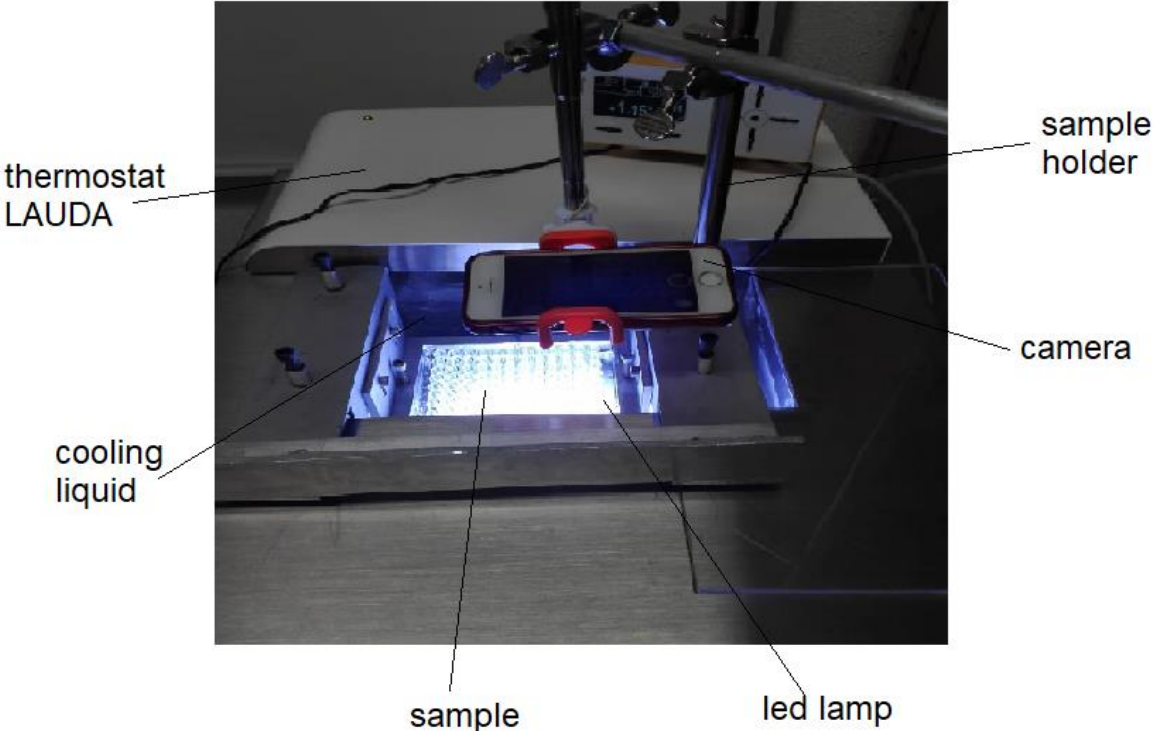


Figure 19. DFA system with a LAUDA thermostat filled with cooling liquid, a light lamp, and a metallic support to hold the camera and the sample.

7.3.4. FREEZING EXPERIMENT



Figure 20. Steps to achieve the freezing assay.

The first step was to sink the led lamp inside the thermostat. The second step was to place the sample in the sample holder (see a. in Figure 20), and submerge it in the cooling liquid. It was necessary to ensure that the refrigerant must be at the same level that the sample contained in the holes as depicted in Figure 21. The third step was to program a temperature ramp to decrease the temperature from 0°C to -40°C in 15 minutes. The experiment was stopped at -40°C because it is well known that below this temperature all the droplets freeze spontaneously by homogenous freezing.⁶⁴ After, the system was covered with a black box (see Figure 20b) to avoid the dispersion of light coming from the led lamp and to avoid the interference of external light in the video recording. Finally, once all the previous steps were performed, the freezing experiment was initiated while the freezing of each hole (droplet) was recorded by the camera.

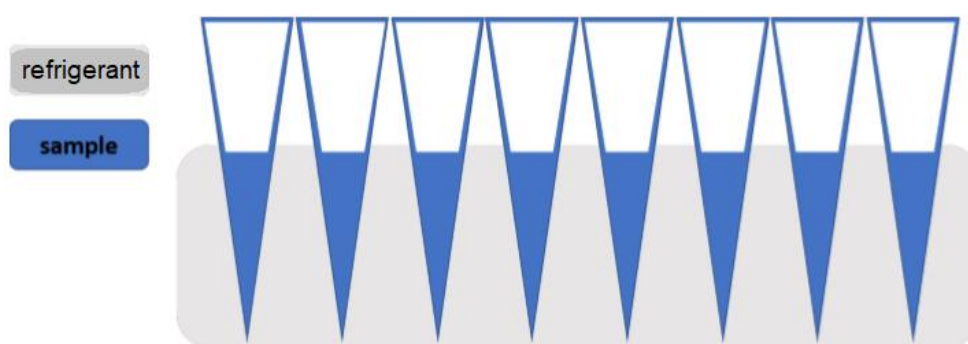


Figure 21. Level of submersion of the Elisa plate in the refrigerant (polydimethylsiloxane), adapted from Cascajo³⁸

7.3.4.1. Standard Analysis

To calibrate the equipment and to determine if the conditions to perform the freezing assays are correct, the first experiment was to analyze deionized water, which should freeze homogeneously because INPs are supposed to be absent. Similarly, a standard of Arizona test dust (ATD) at 0.1% was analyzed because it has been widely studied as its composition is believed to be comparable to that of natural mineral dust. This experiment was conducted with the aim to compare the ice nucleating ability of this standard with literature data.

7.3.5. STATISTICAL ANALYSIS

To analyzed the experiments, the freezing time (t) at which each hole (droplet) froze was obtained from the video, and introduced in seconds in an excel table as Figure 22 shows. The freezing time allowed us to compute the temperature with the help of the next relationship.

$$T = \frac{40^{\circ}\text{C}}{900\text{s}}(t) \quad (1)$$

Where $\frac{40^{\circ}\text{C}}{900\text{s}}$ represents the cooling rate during the temperature ramp. Having the freezing temperature values for the 96 holes, the number of frozen holes in temperature intervals of 0.5°C were counted in order to compute the frozen fraction as a function of temperature. The frozen fraction was calculated by dividing the number of drops (holes) frozen at a given temperature interval to the total number of holes (i.e., 96). Subsequently the cumulative concentration of INPs (C_{INP}) associated to each sample was computed by the next equation.⁶⁵

$$C_{INP}(T) = -\ln(F_{uf}) / V_{drop} \quad (2)$$

where F_{uf} is the fraction of unfrozen droplets at supercooling temperature T , and V_{drop} is the volume of the drop. All the calculations were performed in the excel sheet illustrated below in Figure 22.

Sample	Temp (C)	Temp (C)	Range T (C)	Drop #	Frozen Fraction
A1	0	0	0	0	0
A2	0	0	-0.5	0	0
A3	0	0	-1	0	0
A4	0	0	-1.5	0	0
A5	0	0	-2	0	0
A6	-11.911	0	-2.5	0	0
A7	-11.511	0	-3	0	0
A8	-13.467	0	-3.5	0	0
A9	0	0	-4	0	0
A10	-18.756	0	-4.5	0	0
A11	0	0	-5	0	0
A12	0	0	-5.5	0	0
B1	0	0	-6	0	0
B2	-11.244	0	-6.5	0	0
B3	-18.444	-10.267	-7	0	0
B4	-11.067	-10.267	-7.5	0	0
B5	-11.289	-10.356	-8	0	0
B6	-19.689	-10.533	-8.5	0	0

Freezing time in seconds	A	B	C	D	E	F	G	H
1				237		416		
2		253	245	240	260	241	264	429
3		415	306	254	254	396	231	245
4		249	249	237	233	335	231	250
5		254	250	334	321	277	259	416
6	268	443	251	437	258	250	446	316
7	259	325	253	448	424	287	282	319
8	303	287	380	427	260	467	306	261
9		411	456	262	271	284	321	267
10	422	283	244	255	385	377	474	257
11		298	262	336	283	271	320	454
12			436	261	355	436	468	268

Figure 22. Statistical Analysis of the DFA experiments.

7.3.5.1. Activation Curves

Values of frozen fraction and temperature were plotted by importing and processing the data from Excel in Matlab. Plots where the y-axis is the frozen fraction and x-axis is the experimental temperature range are called activation curves. From these curves, the T_{50} can be reported, where T_{50} refers to the temperature at which 50% of the holes (droplets) froze. Moreover, this value provides information about the ice nucleating ability of the sample and can be used to perform a direct comparison between samples.

7.4. ATOMIC ABSORPTION SPECTROSCOPY

Atomic absorption spectroscopy (AAS) has become a useful technique in the determination of metals and metalloids. AAS works by introducing a sample into an atom cell where it is desolvated and atomized, then a light is emitted by a light source and absorbed by the analyte, where the amount of absorbed light is proportional to the concentration of atoms in the cell.⁶⁶ In this work, a specific type of AAS called Flame Atomic Absorption Spectroscopy (FAAS) is used to measure the concentrations of Na^+ , K^+ , Ca^{2+} , and Mg^{2+} in the rain water samples.

This technique is based on the principle that ground state atoms absorb light in a specific wavelength and thus the decrease of light intensity is measured. Here the metal ions in a solution are converted to the atomic state by means of a flame.⁶⁷

7.4.1. SAMPLE PREPARATION

Standard (Std) solutions concentrations to calibrate the FAAS are shown in Table 6. These solutions were prepared with deionized water and concentrated solutions of Na^+ , K^+ , Ca^{2+} , and Mg^{2+} .

Table 6. Concentrations of the standard solutions used in FAAS experiments.

Metal	Concentration (mg/L)					
	Std 1	Std 2	Std 3	Std 4	Std 5	Std 6
Na^+	0.25	0.50	0.75	1.00	1.50	2.00
K^+	0.10	0.25	0.50	0.75	1.00	-
Ca^{2+}	1.00	2.00	3.00	4.00	-	-
Mg^{2+}	0.20	0.30	0.40	-	-	-

In the Na^+ , K^+ solutions, 1 mL of lanthanum concentrated solution was added, and in Ca^{2+} , Mg^{2+} solutions 1 mL of cesium concentrated solution was added. Samples under analysis were separated in aliquots of 10 mL in beakers of 25 mL (see Figure 23). In the same way that for the standard solutions, 1 mL of lanthanum or 1mL of cesium solutions were added in the samples to analyze Na^+ , K^+ , and Ca^{2+} , Mg^{2+} correspondingly.



Figure 23. Sample preparation for Atomic absorption analysis.

Lanthanum is used to prevent the formation of stable compounds that inhibit the signals such as those coming from the formation of stable refractory compounds, and cesium is added to produce an excess of electrons in the flame, thus inhibiting ionization of the analyte because these flame may cause an appreciable ionization.

7.4.2. EQUIPMENT DESCRIPTION

The equipment GBC 932 AA was implemented to perform FAAS analysis, with the next description based on the user manual for Flame Methods Manual for Atomic Absorption.⁶⁸ The system consists of four parts, specifically a hollow cathode lamp, an atomizer, a monochromator, a detector, and a computer as shown Figure 24 .

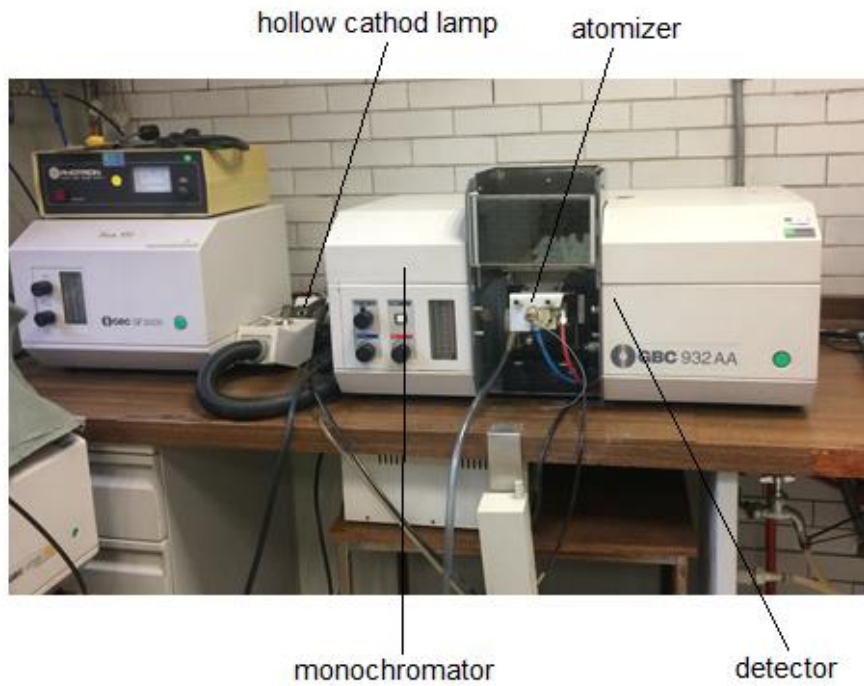


Figure 24. Flame Atomic Absorption Spectroscopy equipment

7.4.2.1. Hollow Cathode Lamps

These type of lamps were used as the radiation source to excite the free atoms in the flame. The lamps are made of a hollow cathode (made of the element under analysis), and a ring anode, which are enclosed in a glass envelope. Furthermore, the lamp is filled of argon or neon (see Figure 25).

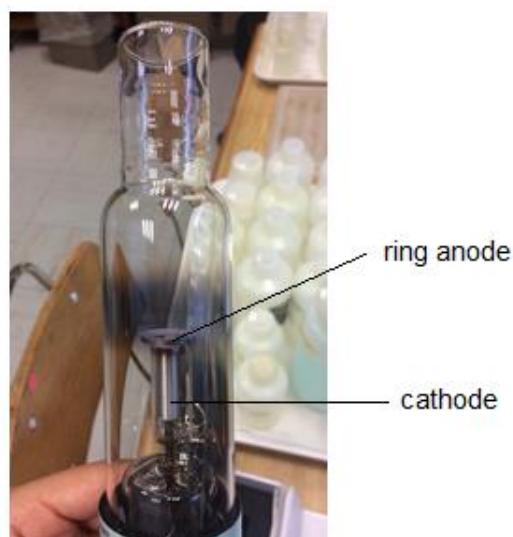


Figure 25. Hollow cathode structure

7.4.2.2. Atomizer

For atomic absorption to occur, the atoms have to be introduced into the excitation beam as free atoms. So, the solvent has to be removed and the chemical bonds broken to form free atoms, this was done by chemical flame. The flame atomizer consists of three major components, a nebulizer (creates vacuum), a spray chamber (classify particles) and a burner. This system converts the liquid into an aerosol, select the correct droplet size (less than $10\mu\text{m}$) and transfer the sample to the burner (of titanium), where atomization occurs. Air acetylene flame is used to create the flame to burn as shown in Figure 26.



Figure 26. Atomizer assembly

7.4.2.3. Monochromator

The monochromator removes the non-desired wavelength in the light beam source to produce a monochromatic light.

7.4.2.4. Detector

A photomultiplier tube is implemented as a detector to read out the information. It works by converting light into an electric signal and then, amplifies that signal.⁶⁹

7.4.3. ATOMIC ABSORPTION ANALYSIS

The initial experiments were done with the standard solutions in order to calibrate the equipment, and then, with the rain water samples from the different locations in the next way: a) The capillary tube connected to the atomizer assembly illustrated in Figure 26 was placed inside the beaker containing the sample, which was aspirated and introduced into the flame. b) In the flame, the sample was desolvated, vaporized, and atomized. c) The hollow cathode lamps emit the light during atomization. d) Emitted light intensity was detected. e) Once the signal had been measured, the capillary tube was washed out with deionized water, and the procedure was repeated for the next sample.

7.4.4. DATA ANALYSIS

A computer connected to the FAAS equipment stored the data of concentrations of the standard solutions and produced linear calibration curves. From these curves, the unknown concentrations of the elements on the samples were derived.

7.5. HYSPLIT BACK-TRAJECTORIES

Hybrid single particle Lagrangian integrated trajectory (HYSPLIT) model was used to compute rainfall trajectories to qualitatively correlate these data with the ice nucleating abilities of rain water samples.⁷⁰

The back-trajectories were performed at latitudes and longitudes corresponding to the sampling locations Quito, CDMX, and ALTZ, at dates and times shown in Table 3, Table 4, and Table 5, and at height values of 50, 250 and 500 m above ground level as shown in Figure 27.

Model Parameters

Trajectory direction: Forward Backward (Change the default start time!) [More info](#)

Vertical Motion: Model vertical velocity Isobaric Isentropic [More info](#)

Start time (UTC): Current time: 19:43
 year: 19 month: 02 day: 04 hour: 19 [More info](#)

Total run time (hours): 24 [More info](#)

Start a new trajectory every: 0 hrs Maximum number of trajectories: 24 [More info](#)

Start 1 latitude (degrees): 19.118700 [More info](#)

Start 1 longitude (degrees): -98.655200 [More info](#)

Start 2 latitude (degrees):

Start 2 longitude (degrees):

Start 3 latitude (degrees):

Start 3 longitude (degrees):

Level 1 height: 50 meters AGL meters AMSL [More info](#)

Level 2 height: 250

Level 3 height: 500

The following options apply only to the GIF, PDF, and PS results (not Google Earth)

Plot resolution (dpi): 96 [More info](#)

Zoom factor: 70 [More info](#)

Plot projection: Default Polar Lambert Mercator [More info](#)

Vertical plot height units: Pressure Meters AGL Theta [More info](#)

Label Interval: No labels 1 hour 6 hours 12 hours 24 hours [More info](#)

Plot color trajectories? Yes No

Use same colors for each source location? Yes No [More info](#)

Plot source location symbol? Yes No

Distance circle overlay: None Auto [More info](#)

U.S. county borders? Yes No [More info](#)

Postscript file? Yes No [More info](#)

PDF file? Yes No

Plot meteorological field along trajectory? Yes No [More info](#)

Note: Only choose one meteorological variable from below to plot

Dump meteorological data along trajectory: [More info](#)

- Terrain Height (m)
- Potential Temperature (K)
- Ambient Temperature (K)
- Rainfall (mm per hr)
- Mixed Layer Depth (m)
- Relative Humidity (%)
- Downward Solar Radiation Flux (W/m**2)

Figure 27. Back-trajectories parameters. ⁷¹

8. RESULTS AND DISCUSSION

8.1. DROPLET FREEZING ASSAY

8.1.1. DETERMINATION OF THE IDEAL CONDITIONS

The ideal conditions to perform all the experiments are presented in **¡Error! No se encuentra el origen de la referencia.** Figure 28a shows the comparison of homogenous freezing on deionized water and heterogeneous freezing on ATD particles. The homogeneous freezing line can be considered as a blank, and therefore, all the freezing events observed at temperatures higher than those represented by this activation curve are attributed to the presence of INPs on the rain samples. Additionally, the activations curves with T_{50} values closer to zero (away from the homogeneous freezing curve), will be considered more efficient to form ice crystals. Figure 28b shows that the presence of chloroform does not affect the ice nucleating abilities of the samples, therefore, the samples from Quito, which contain chloroform are comparable with the samples without chloroform collected in Mexico (CDMX and ALTZ).

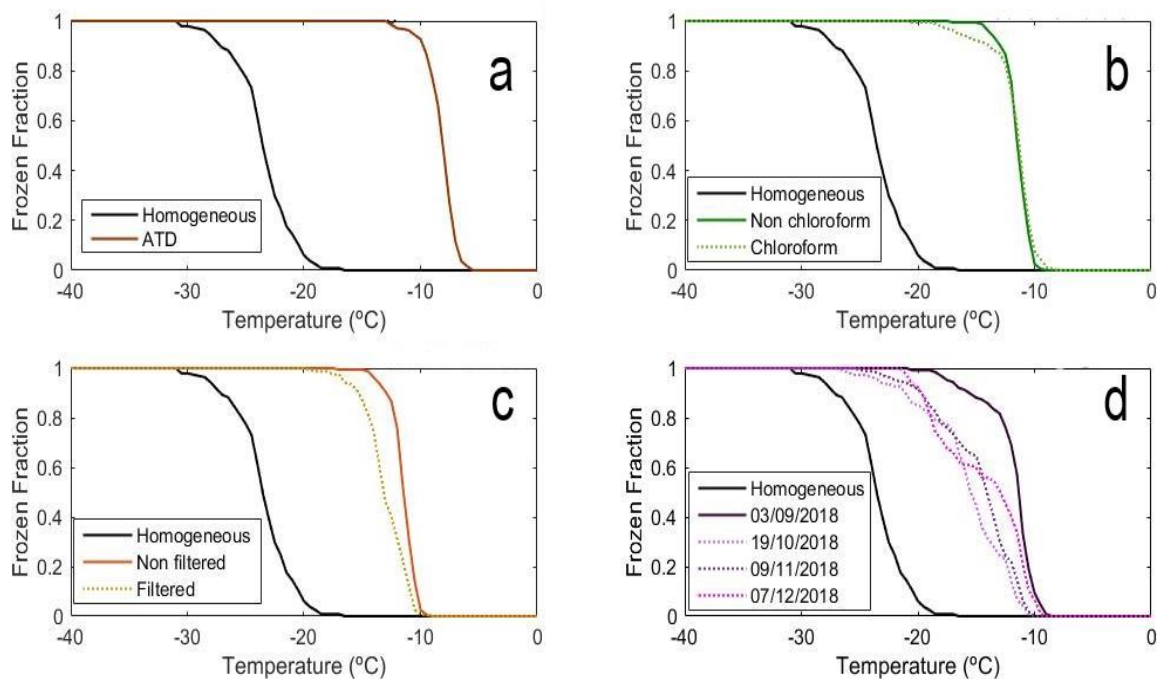


Figure 28. Determination of the ideal conditions for the freezing experiments. a) Working temperature range, b) Chloroform effect, c) Filtration effect, and d) Aging effect on the rain water samples.

For the filtration test (Figure 28c), it can be observed that the efficiency of the rain water sample decreases after filtration, which is consistent with the requirement that good INPs are mostly insoluble as proposed by Pruppacher and Klett.²¹ Also, the aging test shown in Figure 28d indicates that the ice nucleating abilities of the rain water samples is reduced with time, leading to a lower freezing temperatures in a similar way that the decrease in the ice nucleating efficiency of some samples of snow presented in the study of Stopelli et al.⁷² This fact shows that storage time could affect parameters such as temperature activation range, and also the temperature-dependent INPs concentration. Welti et al.⁷³ found a decrease on the number of INPs for aerosol samples collected on filters for a sampling period of four years. It is important to note that the aforementioned studies also used a DFA.

In brief, with the previous information it is found that the ideal conditions to perform freezing experiments in rain water samples through DFA are based on a reduced external manipulation of the samples such as filtering process, in which active material is lost, and storage time of samples, which should be minimized to avoid particle's aging. Even when the nucleating abilities of INPs in the present study were not affected by chloroform at a concentration of 1%, the addition of chemical agents to avoid the increase or decrease of the efficiency of INPs should be prevented.

8.1.2. URBAN CITIES COMPARISON

Figure 29 shows that the samples from both places Quito (blue curves) and CDMX (orange curves) contained aerosol particles with the potential to act as INPs to catalyze the formation of ice particles with temperatures closer to 0°C and far from the homogenous curve.

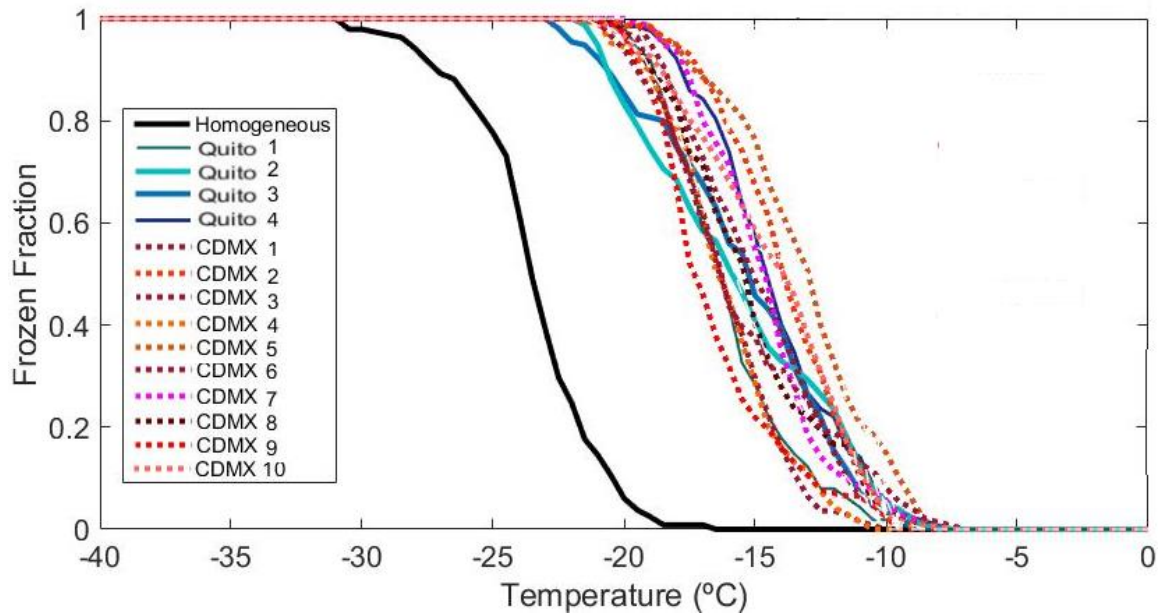


Figure 29. Activation curves from Quito and Mexico City. This figure compares the ice nucleating abilities of the two urban cities through the variation of frozen fraction as a function of temperature. Here, the solid black curve represents the homogenous freezing of deionized water, while the blue set of lines represent the activation curves from Quito samples, and the dotted lines those from Mexico City.

Initially, it was expected to have a higher aerosol particles concentration in CDMX than in Quito because this place presents higher concentrations of inhabitants, vehicles, and industries, those of which could contribute to an increase in the emission of aerosol particles to the atmosphere, thus, there would be a higher concentration of INPs in CDMX than in Quito. Nevertheless, Figure 29 shows that nucleating abilities of rain water samples behaves in a similar way in both urban places.

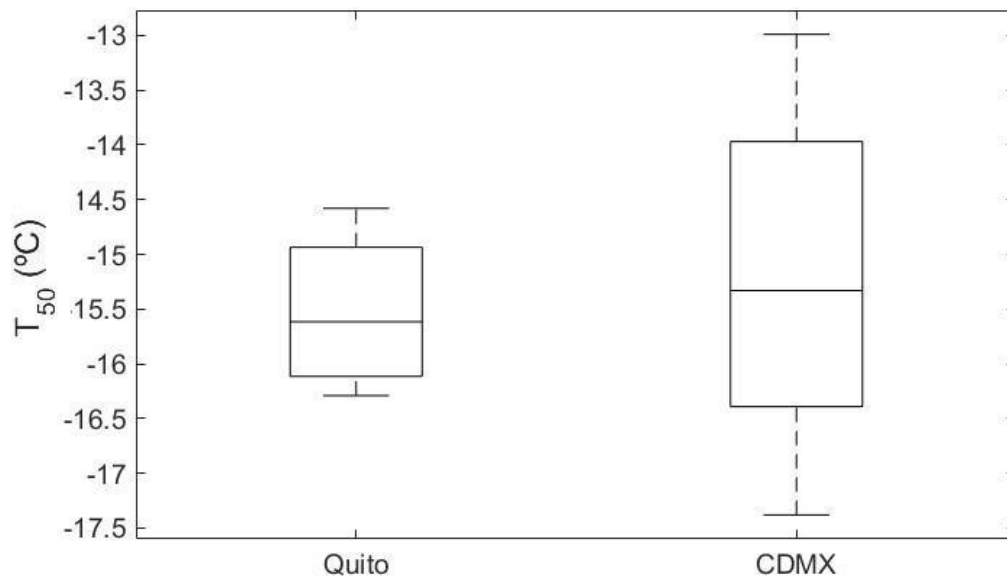


Figure 30. Comparative box-plot of the average value of T_{50} for rain water samples from the urban locations Quito and Mexico City.

The box-plot shown in Figure 30 indicates that in average the nucleating abilities from those places are similar because T_{50} for the CDMX and Quito are almost the same with median values of $-15.43 \pm 0.01^\circ\text{C}$ and $-15.53 \pm 0.01^\circ\text{C}$, respectively. However, the T_{50} reported for CDMX reports higher variability in comparison to Quito which can be related to the amount of samples considering in the analysis, four for Quito and ten for CDMX. Additionally, the variation in the number of samples is an indicative of the sampling time range. The sampling time for Quito only covers one month i.e., June, while for CDMX the sampling time was larger (June to November). The observed variability in the CDMX is in line with the observations made by Bigg⁷⁴, who indicated that the concentration of INPs varies depending on time periods, which will affect the ice nucleating abilities of the samples.

Chen et al.⁷⁵ introduce an analysis of the INPs in Beijing with the global perspective that INPs have not been well examined in terms of urban regions as is the case of this Chinese megacity. The authors found that the INPs collected in filters and submitted to freezing experiments were activated in the range from -6°C to -25°C while the results in the present study shows that INPs on samples from Quito were activated between -8°C to -23°C , and from CDMX in the range of -7°C to -22°C . Additionally, Yadav et al.⁶⁵ found that INPs present in precipitation samples collected in New Delhi (India) are active between -10°C to -22°C . Therefore, the present results are in good agreement with those reported in other densely populated cities.

8.1.3. URBAN VS. RURAL LOCATIONS.

In Figure 31 the rain water samples from a rural location, i.e., ALTZ are compared with the urban cities Quito and CDMX. It is observed that samples from ALTZ contained more efficient INPs given that the ALTZ activation curves are closer to 0°C in comparison to the activation curves from Quito and CDMX (by approximately 5°C at a frozen fraction of 0.5). This fact can be associated in part by the presence of biological particles. Given that ALTZ is a rural place and the monitoring station is surrounded by vegetation it is believed that the biological content on the ALTZ samples is higher in comparison to Quito and CDMX. Biological particles have been shown to be the most efficient INP (especially bacteria), with onset freezing temperatures as high as -2°C.^{20,19}

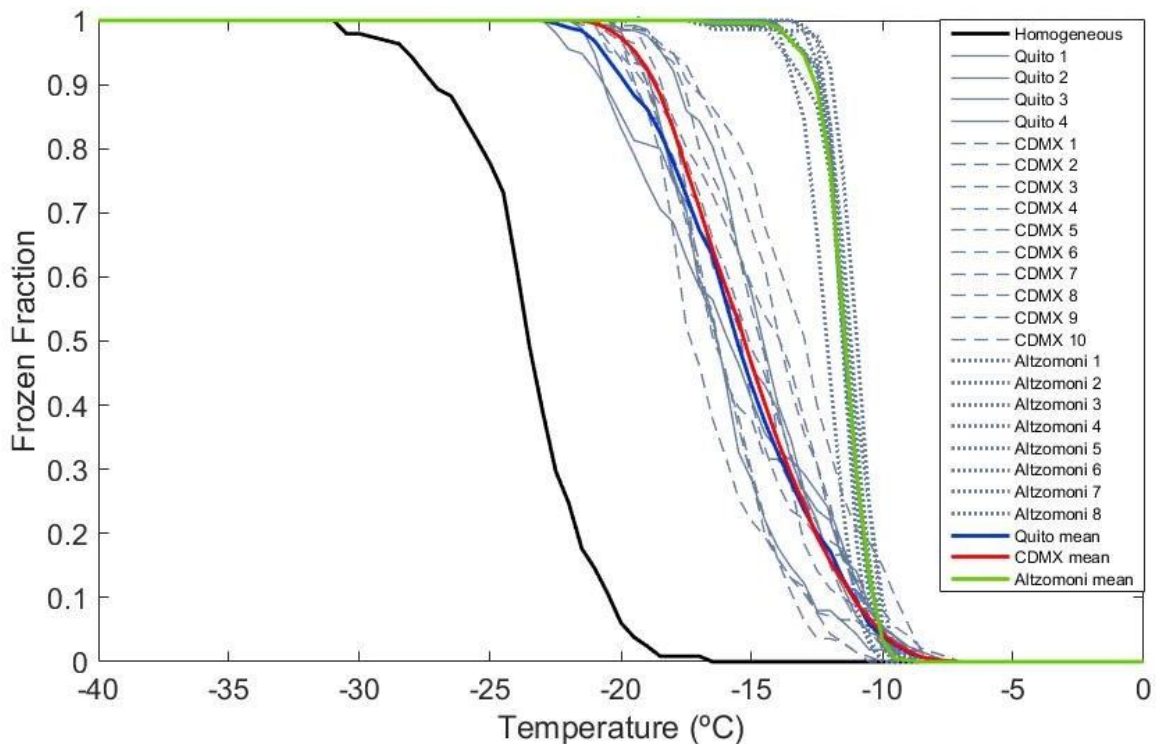


Figure 31. Activation curves from Quito, Mexico City, and Altzomoni. The variation of frozen fraction as a function of temperature for Quito samples are represented by the continuous gray lines, cut lines for Mexico City, and dotted lines for Altzomoni. The average activation curves for Quito, Mexico City, and Altzomoni are represented by the solid blue, red, and green lines, respectively.

Also, ALTZ is compared with other rural locations to analyze the ice nucleating abilities of aerosol particles in those places far from direct anthropogenic emissions. In the study of Conen et al.⁷⁶ atmospheric INPs were collected between 02 and 06 July, 2015 at the Halde

observatory located at 69.92°N and 22.80°E in Norway. The samples collected were submitted to droplet freezing experiments, and it was found that INPs activated in a temperature range from -8°C to -15°C, whereas INPs from ALTZ analyzed in the present study are observed to activate between -9°C to -17°C. Initially, the similar activation temperature range will suggest a relationship between INPs from rural areas, then, to support this hypothesis more studies are introduced such as those of the literature^{77,78}.

Conen et al.⁷⁷ analyze the capacity to nucleate ice of particulate matter with particle diameter of 10 µm or less (PM₁₀) by immersion freezing experiments with samples collected at the High Alpine Research Station Jungfraujoch (4158 m.a.s.l., Switzerland). The authors found that the measured INPs activated between -7°C and -12°C. Furthermore, Creamean et al.⁷⁸ performed a study to determine the marine and terrestrial influence of INPs in an Arctic oilfield location. The authors found a cumulative INP spectra in a temperature range from -5°C to -30°C for different particle sizes. Therefore, a clear tendency between remote places cannot be established because the wide range of contributions of aerosol particles emissions (maritime or terrestrial, and local or external) will affect at different levels the ice nucleating abilities. However, it is noted that remote places are likely influenced by biological particles due to the high freezing temperatures.

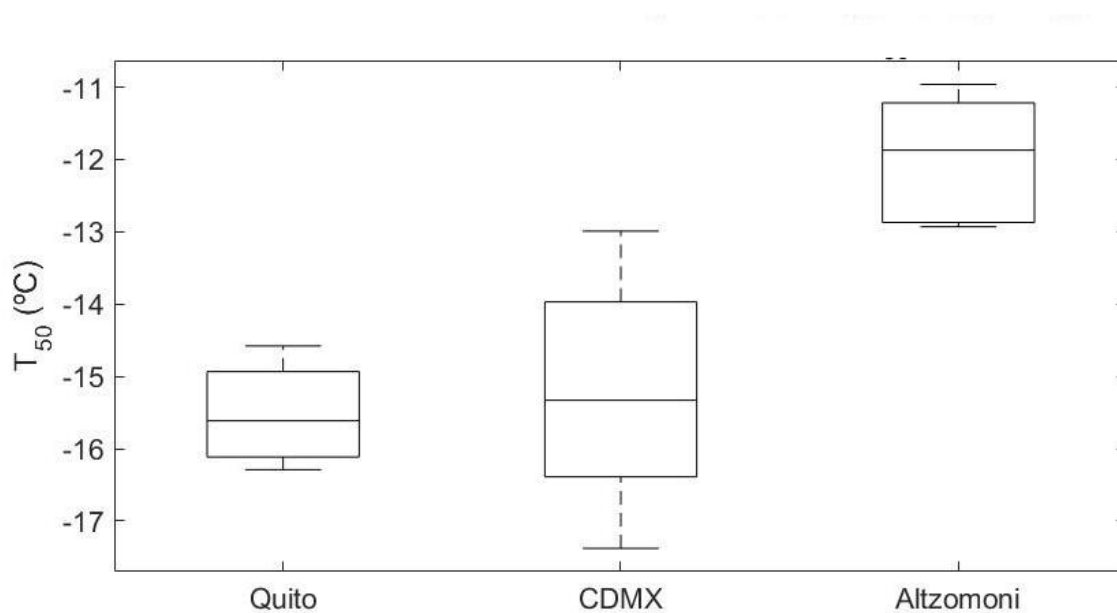


Figure 32. Comparative box-plot of the average value of T_{50} for rain water samples from the three sampling places Quito, Mexico City, and Altzomoni.

A box-plot diagram to compare the variability of samples from the three places under analysis Quito, CDMX, and ALTZ is shown in Figure 32, where the samples from ALTZ report a median value of $11.81 \pm 0.01^\circ\text{C}$, compared with the urban locations reporting a higher T_{50} (i.e., 3.6°C approx.). Then, this figure describes the higher ice nucleating abilities found in rain water samples from ALTZ due to the closeness of the T_{50} to 0°C . Additionally, it is also shown that the T_{50} values from ALTZ has a lower variability, in comparison to CDMX, despite the “large” number of samples and the large covered sampling period (June to November). This could be an indication that the source of the INPs contained in the precipitation samples in ALTZ is the same. This is in contrast with Quito and CDMX where the INPs are likely from the planetary boundary layer, while the INPS measured in ALTZ are likely from the free troposphere.

8.1.4. ICE NUCLEATING PARTICLES CONCENTRATION

From the activation curves shown above and with the help of Equation 2, the INP concentration for each sample was calculated. The data of INPs concentrations from the present study is compared with the data reported³ as shown in Figure 33. The Petters and Wright³ study collected information from the literature associated to INPs concentrations found in different precipitation phenomena such as rain, snow, hail, sleet, and cloud water, which were sampled in northern latitudes such as Louisiana, France, Montana, Antarctica, among others. The INP concentrations found in rain water samples from Quito, CDMX, and ALTZ are represented by continuous lines, while the purple shadow area shows the data from Petters and Wright³.

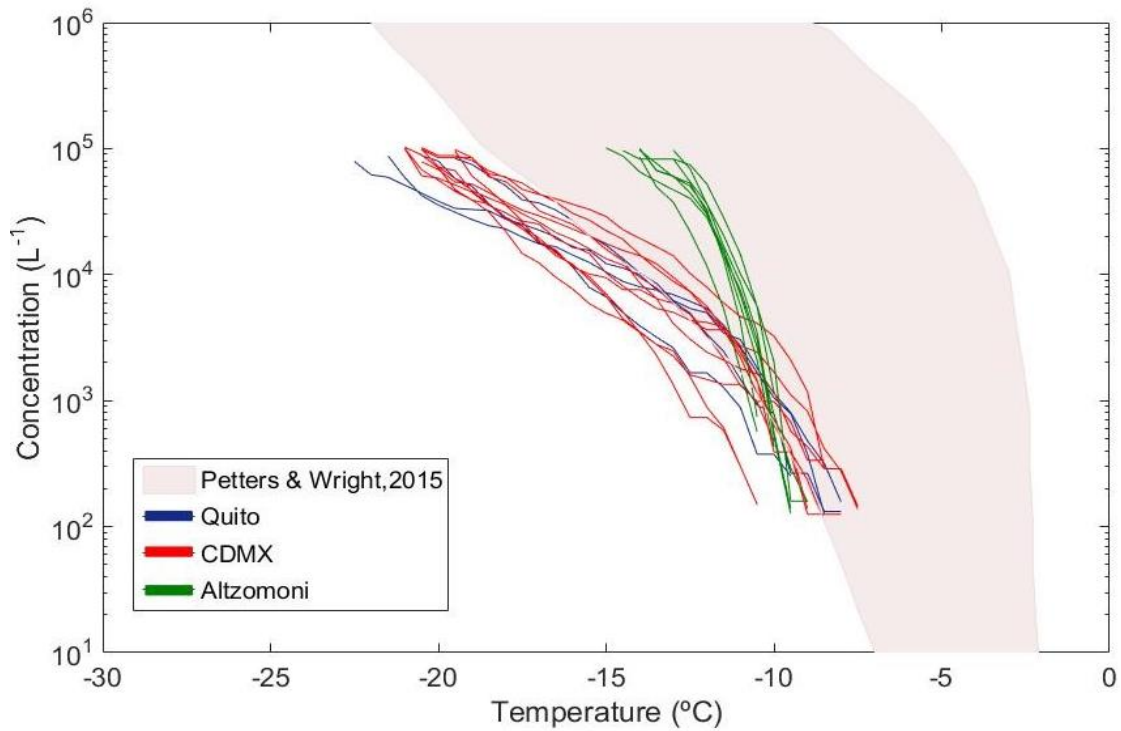


Figure 33. Comparison of INP concentrations obtained experimentally from rain water samples from Quito, Mexico City, and Alzomoni, together with the reported data by Petters and Wright³. The data obtained for tropical latitudes is compared with studies at north latitudes.

It can be observed that the concentrations of INPs for rain water samples from Quito, CDMX, and ALZ are in the range of 10^2 to 10^5 L^{-1} water in agreement with the reported values³. However, comparing the temperature range of the active INPs present in our sampling locations with those of Petters and Wright³, there is displacement of around $5^\circ C$ from the initial ice crystals formation temperature, which shows that INPs present in those places are not as efficient as those reported in the literature. This discrepancy can be partially associated to the

location of the sampling places because Quito, CDMX and ALTZ are located at tropical latitudes, while the rest of the reported studies are at higher latitudes. This is intriguing and deserves further analysis in future studies.

To understand the INPs behaviour in closer latitudes, the INP concentrations from the present study are also compared with those reported in Cape Verde⁷³, in which INPs were collected on filters and then submitted to immersion freezing experiments. In the tropical city of Cape Verde the samples were taken at the atmospheric observatory located at 16.848°N, 24.871°W. It was found that the INP concentrations at this place ranged from 10^{-1} to 10^6 m⁻³ air, equivalent to 10^2 to 10^6 L⁻¹ water considering the conversion implemented by Petters and Wright³ with a value of condensed water content of 0.4gm⁻³, and an activation range between -5°C to -25 °C. Therefore, the Welti et al.⁷³ data are in agreement with the present study, showing that INPs will have similar concentrations and temperature activation range at tropical latitudes.

On the other hand, to support the tendency of a similar behaviour on the ice nucleating abilities for densely populated cities, the concentration of INPs from the CDMX and Quito are also compared with those found in Beijing (China) and New Delhi (India). In the case of Beijing the INPs concentrations range from 10^3 to 10^6 L⁻¹ water (converted considering a condensed water content of 0.4gm⁻³), while for New Delhi it ranges from 10^3 to 10^7 L⁻¹ water. This is in close agreement with the values found in Quito and CDMX where the concentration of INPs varies between 10^2 and 10^5 L⁻¹ water, showing that there are similarities in the concentrations of INPs in densely populated cities and also in the working temperature range.

8.2. ATOMIC ABSORPTION

The chemical composition of the rain water samples from Quito, CDMX and ALTZ is shown in Figure 34 where the concentration of the metal ions Na⁺, K⁺, Mg²⁺, and Ca²⁺ are reported. It is noted that all the samples contain these ions in different concentrations ranging from 0 ppm to 3 ppm. When the three sampling places are compared, rain water samples collected in Quito shows a higher content of the elements Na⁺, K⁺, Mg²⁺, and Ca²⁺, followed by CDMX and ALTZ.

Generally, the presence of these ions in the three places can be associated to mineral dust, which is mainly composed by oxides and carbonates such CaO, CaCO₃, MgCO₃, and other ionic constituents. Nevertheless, the elevated concentrations found in Quito shows the possibility of

additional sources (construction and cement) besides mineral dust. Another possibility of the high concentrations found in Quito could be attributed to the sampling and handling methods used in Quito which differs from those used in CDMX and ALTZ, as described above. It must be considered that not all the samples from CDMX, and ALTZ were evaluated due to the lack of sample volume.

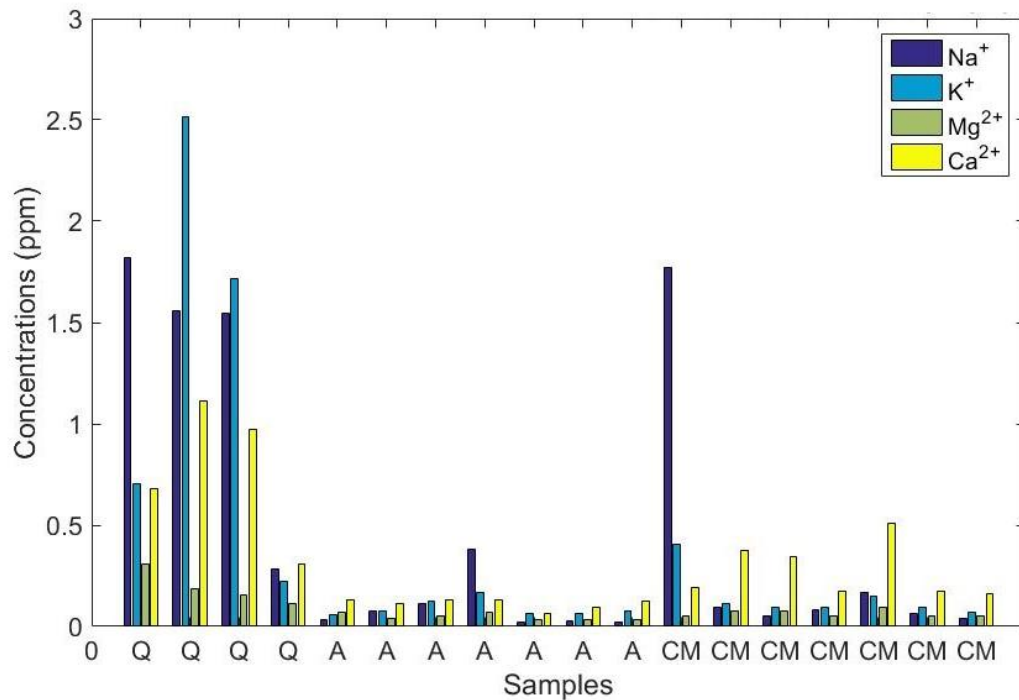


Figure 34. Concentrations of the metal ions Na^+ , K^+ , Mg^{2+} , and Ca^{2+} existing in rain water samples from Quito (Q), Altzomoni (A), and Mexico City (CM). In this graph, the concentrations of ions are compared for the three sampling places, where each ion is represented by a specific color, blue for sodium, sky blue for potassium, green for magnesium, and yellow for calcium.

8.2.1. CORRELATION BETWEEN IONS CONCENTRATION AND T_{50}

Figure 35 shows the correlations of the concentrations of the ions Na^+ , K^+ , Mg^{2+} , and Ca^{2+} with T_{50} , as an indicative of the INPs source. Unfortunately, it is observed that there is not a clear trend between the displayed parameters. Furthermore, the expressed data does not present a good correlation between the chemical composition and the ice nucleating abilities of the samples given that the determination coefficients (R^2) are very low in all the cases (below 0.2.) This fact suggest that atomic absorption spectroscopy provide information about the ionic content of some species in rain water samples such as Na^+ , K^+ , Mg^{2+} , and Ca^{2+} , but not about the efficiency of the them in the formation of ice crystals, which means that high concentrations of these ions are not an indicative of good ice nucleating abilities.

In urban locations the predominant aerosol types are soot, road dust, and secondary organic particles, whereas in urban places biological particles are likely the dominant source. Therefore, it is not surprising that the R^2 values are very low, given that the AA technique is not sensitive to neither biological nor carbonaceous particles.

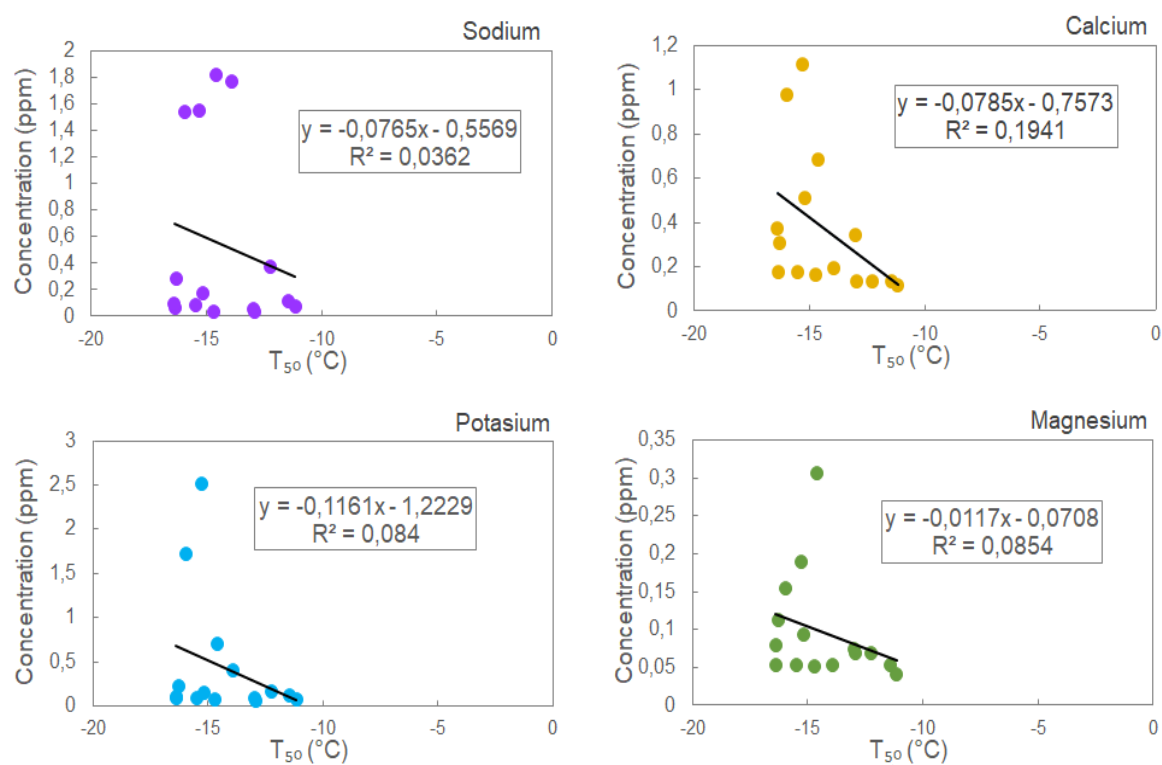


Figure 35. Comparison of metal ions Na^+ , K^+ , Mg^{2+} , and Ca^{2+} concentration determined by flame atomic absorption spectroscopy with the T_{50} values determined by droplet freezing assay.

8.3. BACK-TRAJECTORIES

72 hours Back-trajectories obtained by the NOAA HYSPLIT model are presented below, to see the origin of the air masses at three different altitudes such as 50m, 250m, and 500m during sample collection. The three altitude values were selected to check the uncertainty associated with the topography incorporated in the Hysplit.

8.3.1. QUITO

Figure 36 shows the 72 hours back-trajectories for the most representative sample of Quito with T_{50} of $-15.94 \pm 0.01^\circ\text{C}$ to establish if the influence of local or long-range transport aerosol particles contribution will provide better ice nucleating abilities, which can be related to higher T_{50} values. It is found that this location is influenced by local of air masses only coming from the south, which will be mainly associated to urban dust, soot and organics.

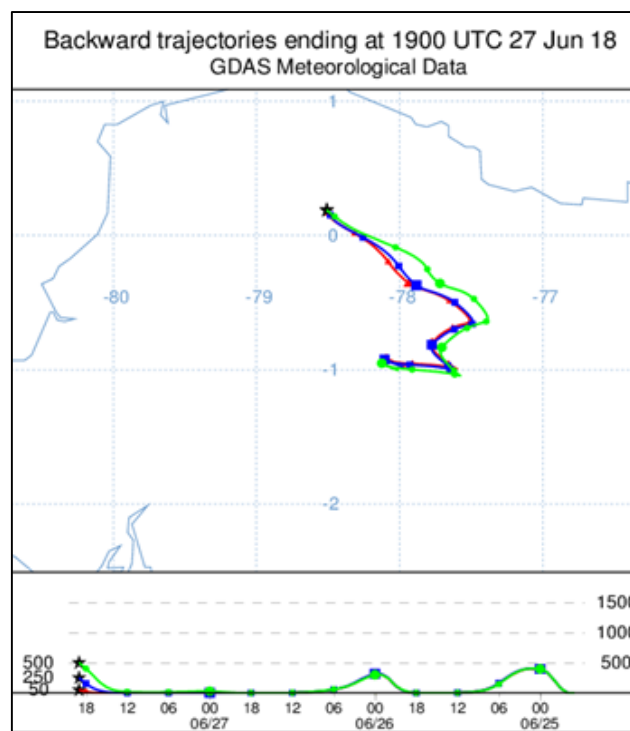


Figure 36. Hysplit backtrajectories performed for Quito rain water sample (QUITO 2) with a T_{50} of $-15.94 \pm 0.01^\circ\text{C}$.

8.3.2. MEXICO CITY

In this case, the analysis represents a rain water sample from CDMX with a T_{50} value of $-15.18 \pm 0.01^\circ\text{C}$ closer to the average value presented for Quito above. Figure 37 shows that CDMX is affected by both local and long-range transport air masses, which can be associated to several sources such as road dust, bioparticles, marine aerosol, organics, etc.

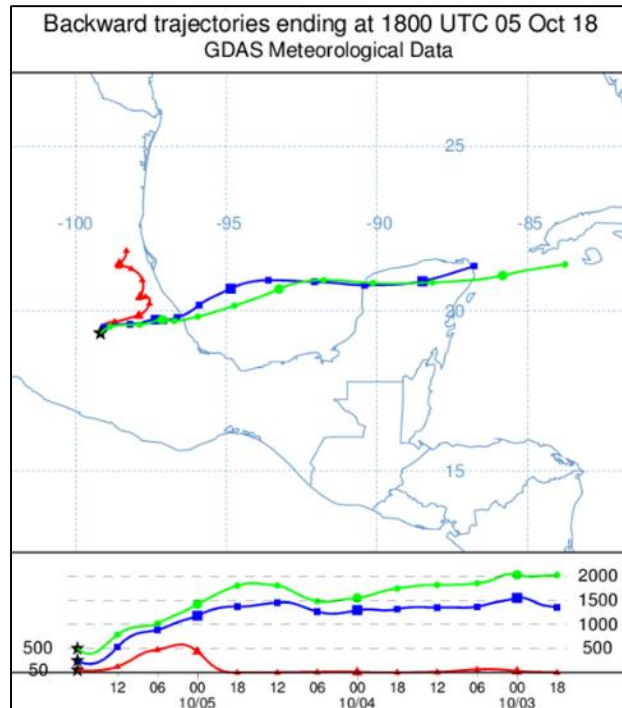


Figure 37. Hysplit backtrajectories performed for CDMX rain water sample (CU3) with a T_{50} of $-15.18 \pm 0.01^\circ\text{C}$.

8.3.3. ALTZOMONI

Figure 38 shows the history of back-trajectories air masses that affect this location. It can be seen that similar to CDMX, ALTZ is highly influenced by local and external air masses. This figure also shows two back-trajectory diagrams for each sample because unlike Quito and CDMX, ALTZ samples were collected in a longer range of time, from the 17 to 21 of October for ALT 7 and from 22 to 28 of October for ALT 8.

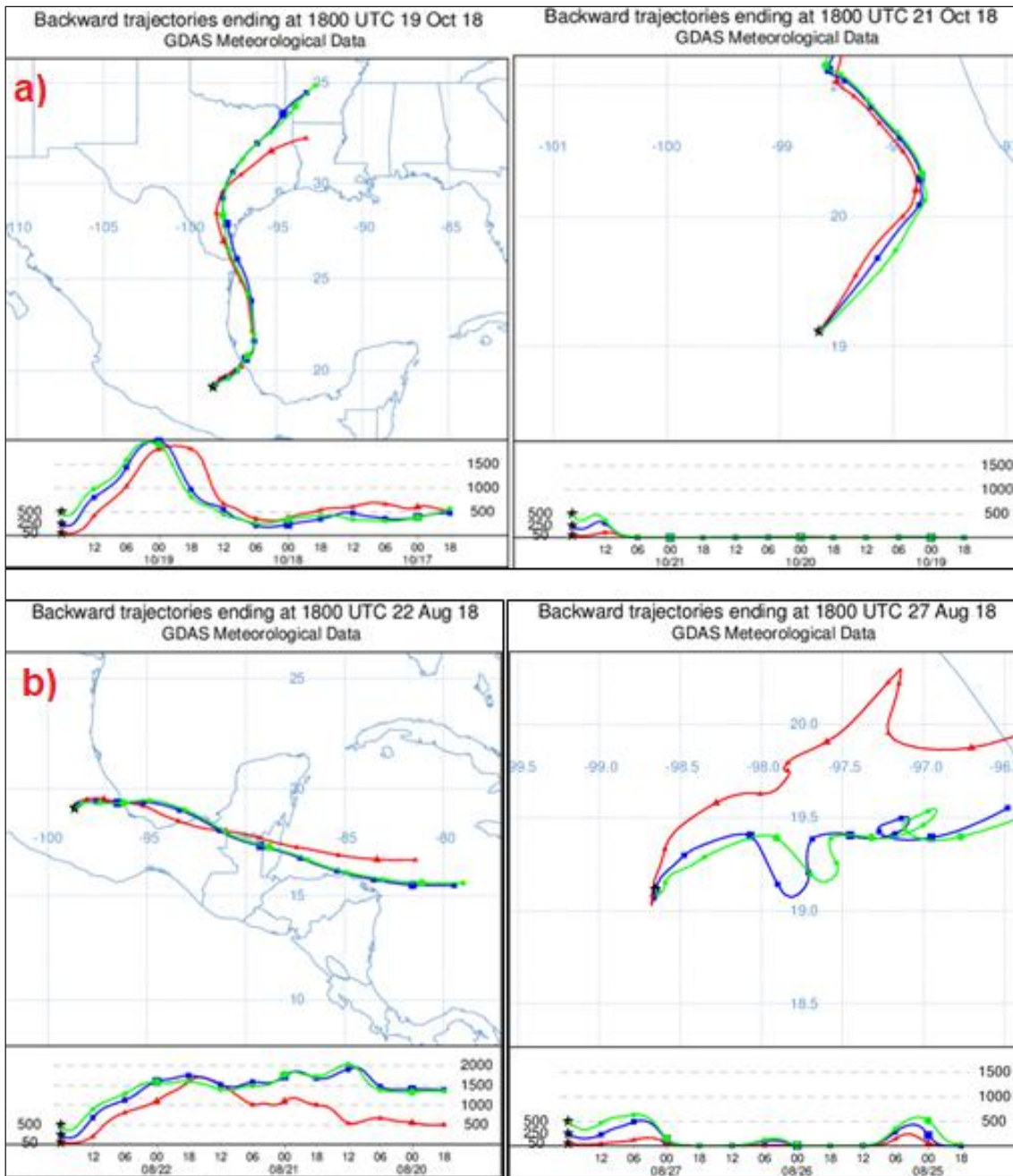


Figure 38. Hysplit backtrajectories performed for Altzomoni rain water samples. a) sample ALT 7 with a T_{50} value of $-11.15 \pm 0.01^\circ\text{C}$. b) sample ALT 8 with a T_{50} value of $-11.49 \pm 0.01^\circ\text{C}$.

9. CONCLUSIONS AND RECOMENDATIONS

9.1. CONCLUSIONS

Three tropical latitude locations Quito, Mexico City and Altzomoni were analyzed in terms of aerosol particles emission and their ability to form ice crystals to understand if there is a pattern in the behavior of ice nucleating particles in the Tropics. In that way, both places Quito and Mexico City were selected by means of population density, urban aerosol contributions and altitude, whereas Altzomoni represented a rural area without direct anthropogenic aerosol particles contributions. To achieve this, rain water samples were collected in the three places, four samples for Quito during June 2018 and ten samples for Mexico City and Altzomoni from June to November 2018. Two experimental techniques, i.e., the DFA and the FAAS were applied to find the concentration of INPs and the concentrations of the ions Na^+ , Ca^{2+} , K^+ , Mg^{2+} , respectively. Furthermore, the HYSPLIT model was used to compute air parcel trajectories and determine possible external and local contributions of aerosol particles.

After performing DFA to analyze the INPs in rain water samples from three tropical places Quito, Mexico City, and Altzomoni it can be concluded that the application of this freezing technique allows the simulation of the heterogeneous immersion freezing mechanism that predominates in mixed-phase clouds, and by which INPs form ice crystals. Moreover, DFA allows us to obtain information about the ice nucleating abilities of aerosol particles given by the parameter of T_{50} , and also the concentrations of these particles acting as precursors in ice formation. It was found that the tree places presented efficient INPs because the freezing temperature values were far from the homogenous curve and closer to zero. Nevertheless, the ice nucleating abilities of INPs from both urban places Quito and Mexico City were not as efficient as those from Altzomoni because the last place is more influenced by the presence of biological particles.

Comparing the results from this research with the literature, a relation between the concentrations of INPs at tropical latitudes was found for the places under analysis and the Cape Verde study, indicating that the concentrations for INPs in the Tropics will range from 10^2 to 10^6 L^{-1} water in an activation temperature range from -5°C to -25°C .

In addition, through the comparison of Quito, Mexico City, Beijing, and New Delhi it was established a tendency in the behavior of INPs in densely populated cities by means of activation

temperature that ranges from -5°C to -30°C . The concentration of INPs in this urban places ranges between 10^2 and 10^7 L^{-1} water. This fact suggests that independently of the aerosol particle emissions, INPs from high dense cities will present similar ice nucleating abilities.

This tendency was not found for remote (rural) places because in those places the high amount of external and local contributions from both natural and anthropogenic aerosol particles emissions, which arrived by global circulation, complicates the determination of activation temperature and INP concentrations.

FAAS analyses provided information about the chemical composition of the rain water samples from Quito, Mexico City and Alzomoni in terms of the concentrations of the ions Na^+ , Ca^{2+} , K^+ , Mg^{2+} . The concentration values of these ions in Quito significantly varied for Mexico City and Alzomoni, which suggest a potential contamination of the samples during the handling and the lack of a proper sampling equipment in the case of Quito. Furthermore, it was determined that even when FAAS derived the concentrations of some ions, there was not a good correlation between the chemical composition of the rain water samples and the ice nucleating abilities of them due to the low values of the determination coefficients obtained when T_{50} and ions concentrations were compared. This implies that FAAS is not a good technique to correlate the chemical composition with the ice nucleating abilities of aerosol particles. Therefore, in order to understand in a better way, the effect of the chemical composition on the capacity of aerosol particles to nucleate ice, other analytical techniques must be used.

Finally, back- trajectories for seventy-two hours of air masses that influenced the three places of interest showed that Quito is only influenced by local aerosol particles, while Mexico City and Alzomoni were highly influenced by local and external contributions in different directions given by the effect of micro, meso, and synoptic scales meteorological phenomena. Combining the information of ice nucleating particles for Quito, Mexico City and Alzomoni and the history of air masses that also contribute with long-range transport particles, it can be concluded that precipitation over continents on high altitude cities (i.e., above 2000 m.a.s.l) are strongly influenced by the presence of INPs independently of their origin (i.e., local or external).

9.2. RECOMMENDATIONS

Based on the knowledge acquired during this project, the following recommendations can be drawn to increase the impact of this type of studies:

- To improve the sampling method in Quito city to avoid any potential contamination on the samples due to particles deposition on the recipient in absence of precipitation, in order to make these samples comparable with those collected in different locations.
- To increase the number of samples and the sampling period for the three sampling places to obtain more information about the behavior of ice nucleating particles in different seasons over the year.
- To execute biological analysis of rain water samples, and also perform a heating test to confirm the presence of biological particles and to determine their efficiency in nucleating ice.
- To analyze other densely populated cities at tropical latitudes to establish a strong pattern of the INPs behavior.

BIBLIOGRAPHY

- (1) Wallace, J. M.; Hobbs, P. V. Atmospheric Science, an Introductory Survey. In *Analysis*; 2006; Vol. 7, pp 153–262. <https://doi.org/10.1007/s007690000247>.
- (2) Seinfeld, J. H.; Pandis, S. N. ATMOSPHERIC CHEMISTRY From Air Pollution to Climate Change; 1998; pp 350–393.
- (3) Petters, M. D.; Wright, T. P. Revisiting Ice Nucleation from Precipitation Samples. *Geophys. Res. Lett.* **2015**, *42* (20), 8758–8766. <https://doi.org/10.1002/2015GL065733>.
- (4) Möhler, O.; DeMott, P. J.; Vali, G.; Levin, Z. Microbiology and Atmospheric Processes: The Role of Biological Particles in Cloud Physics. *Biogeosciences* **2007**, *4* (6), 1059–1071. <https://doi.org/10.5194/bg-4-1059-2007>.
- (5) Rosenfeld, D.; Lohmann, U.; Raga, G. B.; O’Dowd, C. D.; Kulmala, M.; Fuzzi, S.; Reissell, A.; Andreae, M. O. Flood or Drought: How Do Aerosols Affect Precipitation? *Science* (80-.). **2008**, *321* (5894), 1309–1313. <https://doi.org/10.1126/science.1160606>.
- (6) Pryor, S. C.; Crippa, P.; Sullivan, R. C.; Et, A. Atmospheric Chemistry. *Ref. Modul. Earth Syst. Environ. Sci.* **2015**, *2011*, 1–7. <https://doi.org/10.1016/B978-0-12-409548-9.09177-6>.
- (7) Levin, Z.; Cotton, W. R. Aerosol Pollution Impact on Precipitation: A Scientific Review; 2009; pp 1–386. <https://doi.org/10.1007/978-1-4020-8690-8>.
- (8) Seinfeld, J. H. Tropospheric Chemistry and Composition: Aerosols/Particles. *Encycl. Atmos. Sci. Second Ed.* **2015**, *6*, 182–187. <https://doi.org/10.1016/B978-0-12-382225-3.00438-2>.
- (9) Kalberer, M. Aerosols: Aerosol Physics and Chemistry. *Encycl. Atmos. Sci. Second Ed.* **2014**, *1*, 23–31. <https://doi.org/10.1016/B978-0-12-382225-3.00049-9>.
- (10) Lohmann, U.; Lüönd, F.; Mahrt, F. An Introduction to Clouds: From the Microscale to Climate; 2016; pp 115–148. <https://doi.org/10.1017/CBO9781139087513>.
- (11) Jacob, D. Aerosols. In *Introduction to Atmospheric Chemistry*; Princeton University Press, Ed.; 1999; pp 144–152.
- (12) Haywood, J. Atmospheric Aerosols and Their Role in Climate Change; Elsevier B.V., 2015; pp 449–463. <https://doi.org/10.1016/B978-0-444-63524-2.00027-0>.
- (13) Lagzi, I.; Mészáros, R.; Gelybó, G.; Leelössy, Á. Atmospheric Chemistry; 2013; pp 3679–3683.
- (14) Le Roux, G.; Hansson, S. V.; Claustres, A. Inorganic Chemistry in the Mountain Critical Zone: Are the Mountain Water Towers of Contemporary Society Under Threat

- by Trace Contaminants?; Elsevier, 2016; Vol. 21, pp 131–154.
<https://doi.org/10.1016/B978-0-444-63787-1.00003-2>.
- (15) Cotton, W. R.; Yuter, S. Principles of Cloud and Precipitation Formation. *Aerosol Pollut. Impact Precip. A Sci. Rev.* **2009**, 13–43. https://doi.org/10.1007/978-1-4020-8690-8_2.
- (16) Lohmann, U.; Luond, F.; Mahrt, F. *Microphysical Processes in Clouds*; 2016.
- (17) Kanji, Z. A.; Ladino, L. A.; Wex, H.; Boose, Y.; Burkert-Kohn, M.; Cziczo, D. J.; Krämer, M. Overview of Ice Nucleating Particles. *Meteorol. Monogr.* **2017**, 58, 1.1-1.33. <https://doi.org/10.1175/AMSMONOGRAPHS-D-16-0006.1>.
- (18) Vali, G.; DeMott, P. J.; Möhler, O.; Whale, T. F. Technical Note: A Proposal for Ice Nucleation Terminology. *Atmos. Chem. Phys.* **2015**, 15 (18), 10263–10270. <https://doi.org/10.5194/acp-15-10263-2015>.
- (19) Ladino Moreno, L. A.; Stetzer, O.; Lohmann, U. Contact Freezing: A Review of Experimental Studies. *Atmos. Chem. Phys.* **2013**, 13 (19), 9745–9769. <https://doi.org/10.5194/acp-13-9745-2013>.
- (20) Hoose, C.; Möhler, O. Heterogeneous Ice Nucleation on Atmospheric Aerosols : A Review of Results from Laboratory Experiments. *Atmos. Chem. Phys.* **2012**, 9817–9854. <https://doi.org/10.5194/acp-12-9817-2012>.
- (21) Pruppacher, H. R.; Klett, J. D. *Microphysics of Clouds and Precipitation*; 1997; pp 287–355. <https://doi.org/10.1007/978-0-306-48100-0>.
- (22) Field, P. R.; Lawson, R. P.; Brown, P. R. A.; Lloyd, G.; Westbrook, C.; Moisseev, D.; Miltenberger, A.; Nenes, A.; Blyth, A.; Choulaton, T.; et al. Secondary Ice Production - Current State of the Science and Recommendations for the Future. *Meteorol. Monogr.* **2016**, 7.1-7.16. <https://doi.org/10.1175/AMSMONOGRAPHS-D-16-0014.1>.
- (23) Hallett, J.; Mossop, S. Production of Secondary Ice Particles during the Riming Process. *Nature* **1974**, 26–28. <https://doi.org/10.1038/252497a0>.
- (24) Mason, J.; Maybank, J. The Fragmentation and Electrification of Freezing Drops. *J. Atmos. Sci.* **1960**, 176–185. <https://doi.org/https://doi.org/10.1002/qj.49708636806>.
- (25) Vardiman, L. The Generation of Secondary Ice Particles in Clouds by Crystal–Crystal Collision. *J. Atmos. Sci.* **1978**, 35 (11), 2168–2180. [https://doi.org/10.1175/1520-0469\(1978\)035<2168:TGOSIP>2.0.CO;2](https://doi.org/10.1175/1520-0469(1978)035<2168:TGOSIP>2.0.CO;2).
- (26) Bacon, N. J.; Swanson, B. D.; Baker, M. B.; Davis, E. J. Breakup of Levitated Frost Particles. *J. Geophys. Res. Atmos.* **1998**, 103 (D12), 13763–13775. <https://doi.org/10.1029/98JD01162>.

- (27) Ansmann, A.; Tesche, M.; Althausen, D.; Müller, D.; Seifert, P.; Freudenthaler, V.; Heese, B.; Wiegner, M.; Pisani, G.; Knippertz, P.; et al. Influence of Saharan Dust on Cloud Glaciation in Southern Morocco during the Saharan Mineral Dust Experiment. *J. Geophys. Res. Atmos.* **2008**, *113* (4), 1–16. <https://doi.org/10.1029/2007JD008785>.
- (28) Diehl, K.; Wurzler, S. Heterogeneous Drop Freezing in the Immersion Mode: Model Calculations Considering Soluble and Insoluble Particles in the Drops. *J. Atmos. Sci.* **2004**, *61* (16), 2063–2072. [https://doi.org/10.1175/1520-0469\(2004\)061<2063:HDFITI>2.0.CO;2](https://doi.org/10.1175/1520-0469(2004)061<2063:HDFITI>2.0.CO;2).
- (29) DeMott, P. J.; Prenni, A. J.; Liu, X.; Kreidenweis, S. M.; Petters, M. D.; Twohy, C. H.; Richardson, M. S.; Eidhammer, T.; Rogers, D. C. Predicting Global Atmospheric Ice Nuclei Distributions and Their Impacts on Climate. *Proc. Natl. Acad. Sci.* **2010**, *107* (25), 11217–11222. <https://doi.org/10.1073/pnas.0910818107>.
- (30) Hidy, G. Aerosols: An Industrial and Environmental Science; Press, A., Ed.; Florida, 1984; pp 371–438.
- (31) Soulage, G. Methods of Measurement of Ice Nuclei Concentrations. *Pure Appl. Geophys. PAGEOPH* **1965**, *60* (1), 183–188. <https://doi.org/10.1007/BF00874821>.
- (32) Cziczo, D. J.; Ladino, L.; Boose, Y.; Kanji, Z. A.; Kupiszewski, P.; Lance, S.; Mertes, S.; Wex, H. Measurements of Ice Nucleating Particles and Ice Residuals. *Meteorol. Monogr.* **2017**, *58*, 8.1-8.13. <https://doi.org/10.1175/AMSMONOGRAPHS-D-16-0008.1>.
- (33) Koop, T.; Ng, H. P.; Molina, L. T.; Molina, M. J. A New Optical Technique to Study Aerosol Phase Transitions : The Nucleation of Ice from H₂SO₄ Aerosols. *Am. Chem. Soc.* **1998**, 8924–8931. <https://doi.org/10.1021/jp9828078>.
- (34) Hartmann, S.; Niedermeier, D.; Voigtlander, T.; Clauss, R.; Shaw, R.; Wex, H.; Kiselev, A.; Stratmann, F. Homogeneous and Heterogeneous Ice Nucleation at LACIS : Operating Principle and Theoretical Studies. *Atmos. Chem. Phys.* **2011**, 1753–1767. <https://doi.org/10.5194/acp-11-1753-2011>.
- (35) Lacher, L.; Lohmann, U.; Boose, Y.; Zipori, A.; Herrmann, E.; Bukowiecki, N.; Steinbacher, M.; Kanji, A. The Horizontal Ice Nucleation Chamber HINC : INP Measurements at Conditions Relevant for Mixed-Phase Clouds at the High Altitude Research Station Jungfraujoch. *Atmos. Chem. Phys.* **2017**, No. May, 1–49. <https://doi.org/10.5194/acp-2017-474>.

- (36) Bigg, E. K. The Formation of Atmospheric Ice Crystals by the Freezing of Droplets. *Q. J. R. Meteorol. Soc.* **1953**, 79 (342), 510–519. <https://doi.org/10.1002/qj.49707934207>.
- (37) Vali, G. Sizes of Atmospheric Ice Nuclei. *Nature* **1966**, 2 (2), 407–408. <https://doi.org/10.1038/211676a0>.
- (38) Cascajo, M. Morphology and Dynamics of Ice Crystals and the Effect of Proteins. (Doctoral Dissertation), University of the Basque Country, Department of Physic. España, 2017.
- (39) DeMott, P. J.; Hill, T. C. J.; Petters, M. D.; Bertram, A. K.; Tobo, Y.; Mason, R. H.; Suski, K. J.; Mccluskey, C. S.; Levin, E. J. T.; Schill, G. P.; et al. Comparative Measurements of Ambient Atmospheric Concentrations of Ice Nucleating Particles Using Multiple Immersion Freezing Methods and a Continuous Flow Diffusion Chamber. *Atmos. Chem. Phys.* **2017**, 11227–11245. <https://doi.org/https://doi.org/10.5194/acp-17-11227-2017> ©.
- (40) Tobo, Y. An Improved Approach for Measuring Immersion Freezing in Large Droplets over a Wide Temperature Range. *Sci. Rep.* **2016**, 6, 1–9. <https://doi.org/10.1038/srep32930>.
- (41) Rogers, R. R.; Vali, G. Recent Developments in Meteorological Physics. *Phys. Rep.* **1978**, 2 (2), 65–177.
- (42) WMO. *International Cloud Atlas. Volume I: Manual on the Observation of Clouds and Other Meteors*; 1975; Vol. I. <https://doi.org/10.1371/journal.pone.0144369>.
- (43) Mölders, N.; Kramm, G. Clouds and Precipitation. *Lect. Meteorol.* **2014**, 107–147. <https://doi.org/10.1007/978-3-319-02144-7>.
- (44) Shupe, M. D.; Daniel, J. S.; de Boer, G.; Eloranta, E. W.; Kollias, P.; Long, C. N.; Luke, E. P.; Turner, D. D.; Verlinde, J. A Focus on Mixed-Phase Clouds. *Bull. Am. Meteorol. Soc.* **2008**, 89 (10), 1549–1562. <https://doi.org/10.1175/2008BAMS2378.1>.
- (45) De Boer, G.; Morrison, H.; Shupe, M. D.; Hildner, R. Evidence of Liquid Dependent Ice Nucleation in High-Latitude Stratiform Clouds from Surface Remote Sensors. *Geophys. Res. Lett.* **2011**, 38 (1), 1–5. <https://doi.org/10.1029/2010GL046016>.
- (46) Korolev, A.; McFarquhar, G.; Field, P. R.; Franklin, C.; Lawson, P.; Wang, Z.; Williams, E.; Abel, S. J.; Axisa, D.; Borrmann, S.; et al. Ice Formation and Evolution in Clouds and Precipitation: Measurement and Modeling Challenges. Chapter 5: Mixed-Phase Clouds: Progress and Challenges. *Meteorol. Monogr.* **2017**, 1724, 5.1–5.40. <https://doi.org/10.1175/AMSMONOGRAPHS-D-17-0001.1>.

- (47) Quante, M. The Role of Clouds in the Climate System. *J. Phys.* **2004**, *114*, 1–21. <https://doi.org/10.1051/jp4:2004121003>.
- (48) Aguado, E.; Burt, J. Understanding Weather and Climate; Pearson, P., Ed.; 2007; pp 120–190.
- (49) Rast, M.; Johannessen, J.; Mauser, W. Review of Understanding of Earth's Hydrological Cycle: Observations, Theory and Modelling. *Surv. Geophys.* **2014**, 491–510. <https://doi.org/DOI 10.1007/s10712-014-9279-x>.
- (50) Korolev, A.; Isaac, G. Phase Transformation of Mixed-Phase Clouds. *Q. J. R. Meteorol. Soc.* **2003**, *129* (587 PART A), 19–38. <https://doi.org/10.1256/qj.01.203>.
- (51) Korolev, A.; Field, P. R. The Effect of Dynamics on Mixed-Phase Clouds: Theoretical Considerations. *J. Atmos. Sci.* **2008**, *65* (1), 66–86. <https://doi.org/10.1175/2007JAS2355.1>.
- (52) Mülmenstädt, J.; Sourdeval, O.; Delanoë, J.; Quaas, J. Frequency of Occurrence of Rain from Liquid-, Mixed-, and Ice-Phase Clouds Derived from A-Train Satellite Retrievals. *Geophys. Res. Lett.* **2015**, 6502–6509. <https://doi.org/10.1002/2015GL064604>.It.
- (53) Wegener, A. Thermodynamik Der Atmosphäre. Leipzig, Germany: Barth. 1911.
- (54) Bergeron, T. Über Die Dreidimensional Verknüpfende Wetteranalyse. *Geofys. Publikasj.* **1928**, 111.
- (55) Findeisen, W. Colloidal Meteorological Processes in the Formation of Precipitation. *Meteorol.Z* **1938**, *24* (4), 443–454. <https://doi.org/10.1127/metz/2015/0675>.
- (56) Storelvmo, T.; Tan, I. The Wegener-Bergeron-Findeisen Process - Its Discovery and Vital Importance for Weather and Climate. *Meteorol. Zeitschrift* **2015**, *24* (4), 455–461. <https://doi.org/10.1127/metz/2015/0626>.
- (57) Knopf, D. A.; Wang, B.; Laskin, A.; Moffet, R. C.; Gilles, M. K. Heterogeneous Nucleation of Ice on Anthropogenic Organic Particles Collected in Mexico City. *Geophys. Res. Lett.* **2010**, *37* (11), 1–5. <https://doi.org/10.1029/2010GL043362>.
- (58) Ladino, L. A.; Raga, G. B.; Alvarez-Ospina, H.; Andino-Enriquez, M. A.; Rosas, I.; Salinas, E.; Martínez, L.; Miranda, J.; Ramírez-Díaz, Z.; Figueroa, B.; et al. The Importance of Biological Particles to the Ice Nucleating Particle Concentration in a Coastal Tropical Site. *Atmos. Chem. Phys. Discuss.* **2018**, No. December, 1–26. <https://doi.org/10.5194/acp-2018-1215>.
- (59) RUOA. Meteorological Conditions <https://www.ruoa.unam.mx/index.php?page=home>.
- (60) Juarez, J. Determinación de Las Habilidades de La Microcapa Superficial Del Océano

- Para La Formacion de Cristales de Hielo: Golfo de México vs. Pacífico Norte. (Undergraduated Dissertation), National Autonomous University of Mexico. Atmospheric Science Center. Mexico, 2019.
- (61) Brinkmann, L. LAUDA PRO RP 1090 https://www.lauda-brinkmann.com/products/summary.php?p=PRO_RP_1090.
- (62) GMBH, W. Instrucciones de Servicio: Termostatos de Baño y Termostatos de Circulación PRO; Germany, 2015; pp 1–152.
- (63) RUIJIANG-GROUP. Dimethyl Silicone Oil RJ-201 http://www.ruisilicone.com/Silicone_Fluids/Dimethyl_Silicone_Fluid_Food_Grade.html?gclid=EAIaIQobChMI9cOW7qPX3wIVTAOGCh3PZwSLEAAYASAAEgJU_vD_BwE.
- (64) Koop, T.; Luo, B.; Tsias, A.; Peter, T. Water Activity as the Determinant for Homogeneous Ice Nucleation in Aqueous Solutions. *Nature* **2000**, No. 1, 611–614. <https://doi.org/10.1038/35020537>.
- (65) Yadav, S.; Venezia, R. E.; Paerl, R. W.; Petters, M. D. Sources of Ice Nucleating Particles Over Northern India : Pollution , Dust , or Bioaerosol ? *Environ. Sci. Technol.* **2018**, 1–23.
- (66) Hill, S. J.; Fisher, A. S. Atomic Absorption, Methods and Instrumentation. *Encycl. Spectrosc. Spectrom.* **2010**, No. 1998, 46–53. <https://doi.org/10.1016/B978-0-12-374413-5.00099-3>.
- (67) Faculty of Science and Technology. *Flame Atomic Absorbition Spectroscopy (FAAS)*; 1859.
- (68) Antanasopoulos, N. FLAME METHODS MANUAL FOR ATOMIC ABSORPTION; Australia; pp 1–30. <https://doi.org/10.1145/2505515.2507827>.
- (69) Marmonier, C. Photomultiplier Tubes Principles & Applications; France, 2002; pp 1–15.
- (70) Stein, A.; Draxler, R.; Stunder, B.; Cohen, M.; Ngan, F. NOAA’s HYSPLIT Atmospheric Transport and Dispersion Modeling System, *Bull.* **2015**, 2059–2077. <https://doi.org/http://dx.doi.org/10.1175/BAMS-D-14-00110.1>.
- (71) NOAA. HYSPLIT Trajectories https://ready.arl.noaa.gov/HYSPLIT_traj.php.
- (72) Stopelli, E.; Conen, F.; Zimmermann, L.; Alewell, C.; Morris, C. E. Freezing Nucleation Apparatus Puts New Slant on Study of Biological Ice Nucleators in Precipitation. *Atmos. Meas. Tech.* **2014**, 129–134. <https://doi.org/10.5194/amt-7-129-2014>.

- (73) Welti, A.; Müller, K.; Fleming, Z. L.; Stratmann, F. Concentration and Variability of Ice Nuclei in the Subtropical Maritime Boundary Layer. *Atmos. Chem. Phys.* **2018**, 5307–5320. <https://doi.org/10.5194/acp-18-5307-2018>.
- (74) Bigg, E. K. A Long Period Fluctuation in Freezing Nucleus Concentrations. *J. Meteorol.* **1958**, 561–562.
- (75) Chen, J.; Wu, Z.; Augustin-bauditz, S.; Grawe, S.; Hartmann, M.; Pei, X.; Liu, Z. Ice-Nucleating Particle Concentrations Unaffected by Urban Air Pollution in Beijing , China. *Atmos. Chem. Phys.* **2018**, 3523–3539. <https://doi.org/10.5194/acp-18-3523-2018>.
- (76) Conen, F.; Stopelli, E.; Zimmermann, L. Clues That Decaying Leaves Enrich Arctic Air with Ice Nucleating Particles. *Atmos. Environ.* **2016**, 129, 91–94. <https://doi.org/10.1016/j.atmosenv.2016.01.027>.
- (77) Conen, F.; Henne, S.; Morris, C. E.; Alewell, C. Atmospheric Ice Nucleators Active ≥ -12 °C Can Be Quantified on PM10 Filters. *Atmos. Meas. Tech.* **2012**, 321–327. <https://doi.org/10.5194/amt-5-321-2012>.
- (78) Creamean, J. M.; Kirpes, R. M.; Pratt, K. A.; Spada, N. J.; Maahn, M.; De, G. Marine and Terrestrial Influences on Ice Nucleating Particles during Continuous Springtime Measurements in an Arctic Oilfield Location. *Atmos. Chem. Phys.* **2018**, 18023–18042. <https://doi.org/10.5194/acp-18-18023-2018>.